From labelled to the optimal clinical dose: model-informed dose optimization in medical oncology practice

Tan, Z.

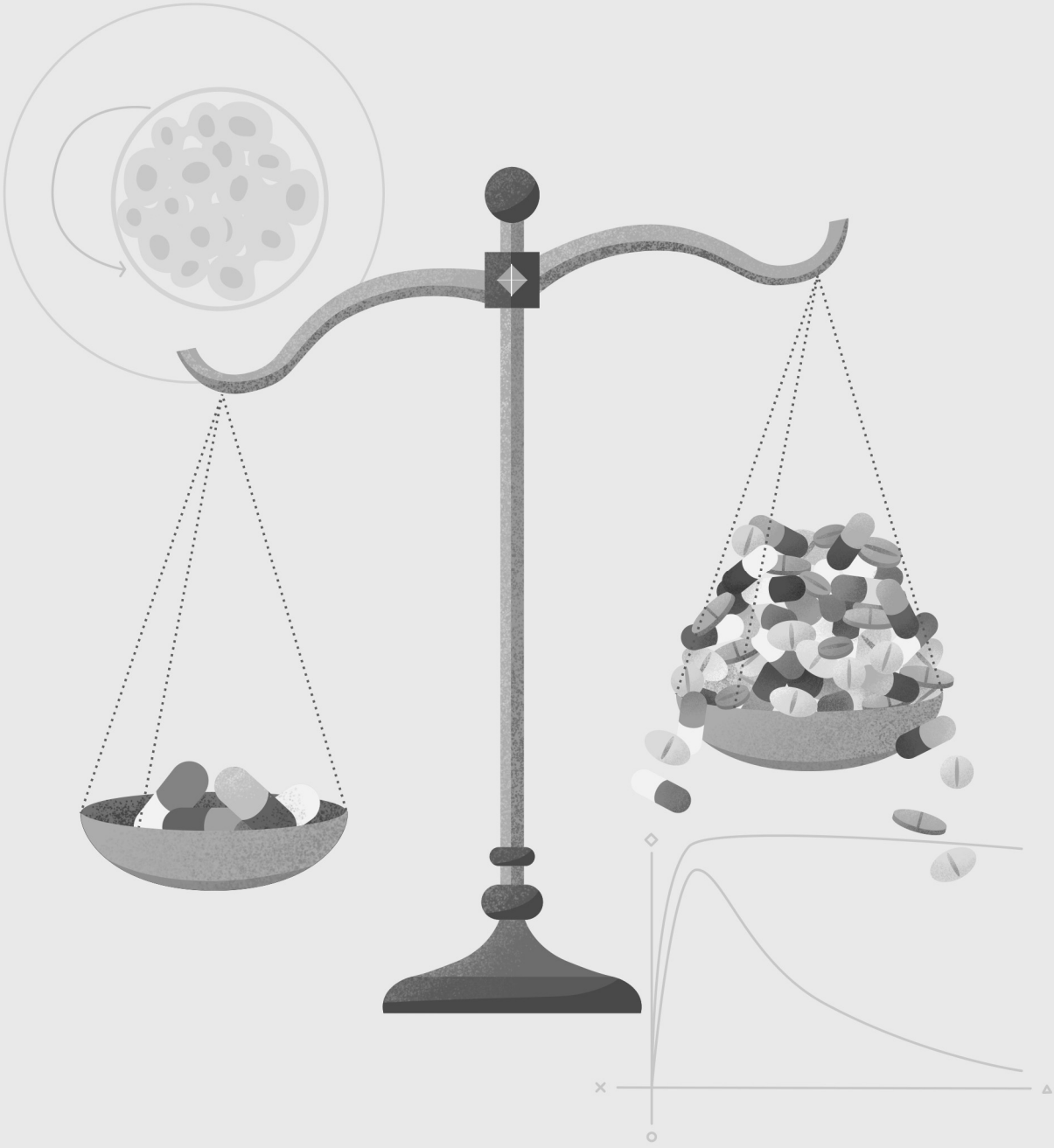

Chapter 4

Model-informed dose optimization of pazopanib in real-world patients with cancer

Zhiyuan Tan, Swantje Völler, Anyue Yin, Amy Rieborn, Hans Gelderblom, Tom van der Hulle, Catherijne A. J. Knibbe, Dirk Jan A. R. Moes

Clin Pharmacokinet 64, 715-728 (2025)

ABSTRACT

Background: Pazopanib is approved for metastatic renal cell carcinoma (mRCC) and soft tissue sarcoma (STS) with 800 mg once daily (QD) taken under fasted conditions. Approximately 60% of patients require dose reductions due to toxicity, with severe liver toxicity necessitating treatment interruptions in over 10% of cases. While a trough concentration ($C_{min,ss}$) target of ≥ 20.5 mg/L has been established for mRCC efficacy, no specific threshold exists for liver toxicity.

Objectives: To develop a population PK, an exposure-liver toxicity and an exposure-tumor size dynamics model to optimize pazopanib initial dose in real-world patients.

Methods: 135 patients were included with median starting dose of 800 mg (IQR 600–800 mg) QD pazopanib fasted with a median follow-up of 120 (IQR 63–372) days. A population pharmacokinetic model was developed using 460 PK measurements from 135 patients. Liver toxicity model was developed with time-to-event modeling and tumor size model was developed using baseline and post-treatment tumor size measurements from 111 patients.

Results: The liver toxicity model, with 27 cases of Grade ≥ 2 liver toxicity out of 135 patients (20%), identified a $C_{min,ss}$ threshold of > 34 mg/L associated with a 3.35-fold increased toxicity risk ($p < 0.01$). An initial dose of 600 mg QD significantly reduced liver toxicity risk ($p < 0.001$) while maintaining $C_{min,ss}$ ≥ 20.5 mg/L for 76% of the simulated individuals. For tumor size dynamics model, tumor growth and decay rates differed between mRCC and STS but showed no pazopanib exposure dependency across the studied range, suggesting maximal tumor inhibition at current exposure levels.

Conclusion: These findings suggest that an initial pazopanib dose of 600 mg fasted, followed by model-informed precision dosing to maintain $C_{min,ss}$ between 20–34 mg/L, may improve efficacy-toxicity balance and mitigate treatment interruptions.

Key words: Pazopanib, pharmacokinetics, modeling and simulation, toxicity, tumor size dynamics, renal cell carcinoma, soft tissue sarcoma

1. INTRODUCTION

Pazopanib is a tyrosine kinase inhibitor (TKI) against vascular endothelial growth factor receptor (VEGFR).[1] In 2009, it was approved for the treatment of patients with metastatic renal cell carcinoma (mRCC).[2] To date, several guidelines recommend pazopanib for use as single agent or combined with PD-1 inhibitors in first-line treatment for mRCC.[3, 4] In 2012, it was also approved for patients with advanced soft tissue sarcoma (STS) who received prior chemotherapy.[5]

A fixed 800 mg fasted daily dose is the registered dose that is recommended for all patients, regardless of the tumor type.[6] It has been suggested that the efficacy of pazopanib is related to the steady state trough concentration ($C_{min,ss}$). A $C_{min,ss} \geq 20.5$ mg/L was associated with improved progression-free survival (PFS, i.e. 19.6 vs. 52.0 weeks, $p = 0.004$) and tumor shrinkage in a retrospective analysis in 177 patients with mRCC.[7] Therefore, a newly published therapeutic drug monitoring (TDM) guideline[8] recommends that pazopanib dose selection should be supported by model-informed precision dosing (MIPD), targeting plasma $C_{min,ss} \geq 20.5$ mg/L.[7] However, there is no information about the target $C_{min,ss}$ in STS patients, nor about thresholds for toxicity of pazopanib.

In a renal cell carcinoma patient population, the incidence of increased mean arterial blood pressure (MAP), diarrhea, hair color change, alanine aminotransferase (ALT) increase, stomatitis, and hand-foot syndrome increased as the plasma pazopanib concentrations increased, with the highest incidence occurring in the fourth $C_{min,ss}$ quartile.[7] Among these toxicities, the most common adverse events related to pazopanib are liver toxicities like aspartate transaminase (AST) and ALT elevations,[9] which lead to dose reductions for mild elevations, and to drug discontinuation for severe elevations. In the pazopanib drug label, liver toxicity was emphasized with a black box warning because around 60% of the patients included in the registration study developed liver toxicity and 12% of the patients experienced severe liver enzyme elevations.[10] A similar incidence was also observed in real-world practice where 40–60% of the patients experienced liver toxicity when treated with pazopanib.[11] So far, only a correlation of Common Terminology Criteria for Adverse Events (CTCAE) grade ≥ 3 overall toxicity, which is also phrased as severe toxicity, and pazopanib exposure was established for mRCC patients, which is $C_{min,ss} < 46–50$ mg/L.[12, 13]

MIPD is a concept that employs mathematical models to design personalized dosing strategies.[14] The benefit of MIPD for targeted therapy has been confirmed by different

studies[15, 16] while no study for pazopanib has been reported yet. Therefore, the objectives of this study are to (i) Develop a POPPK model using drug concentrations obtained during TDM in real-world practice; (ii) Explore pazopanib exposure-liver toxicity relationship in RCC and STS patients; (iii) Explore pazopanib exposure-tumor size relationship for the two tumor types. Ultimately, these efforts will result in an optimized initial dose of pazopanib resulting in optimal efficacy-safety balance.

2. METHODS

2.1. Patients and data collection

2.1.1. PK data

Pazopanib plasma concentration measurements were obtained from patients diagnosed with mRCC or STS who received treatment at Leiden University Medical Center (LUMC) between February 2014 and July 2022. These data were identified from the hospital electronic patient dossier system (HiX, Chipsoft B.V. Amsterdam) and retrieved using the Clinical Data Collector tool (CTcue; v3.1.0, CTcue B.V., Amsterdam, The Netherlands). The bioanalytical assay used was a validated liquid chromatography-mass spectrometry method according to EMA guidelines with a precision (Coefficient of Variation, CV%) of 2.4% and an accuracy of 11%.[17] Patients needed to have at least one pazopanib PK measurement during the treatment. Samples with time after the last pazopanib intake (TAD) between 20–28 hour were defined as trough concentration. Patients' demographic information, including age, sex, body mass index (BMI), weight, height, tumor type was also collected for covariate analysis. TDM routine was performed for each individual and the dose adjustment algorithm was depicted in Supplemental Figure S4.1.

2.1.2. Liver toxicity data

The laboratory assessment data was obtained with CTcue and consists of the relevant liver enzymes ALT, AST and Alkaline phosphatase (ALP). These laboratory assessment data were extracted for the included patients between their start and end day of pazopanib use. Toxicity event was defined as CTCAE (V5.0)[18] Grade ≥ 2 ALT or AST or ALP elevation.

2.1.3. Tumor size data

Tumor size was defined as the sum of longest diameter (SLD) of target lesions, using RECIST 1.1 criteria.[19] Individual lesions records were retrieved from computed tomography (CT) scans in the electronic patient dossier. Patients who did not have available baseline tumor size data were excluded.

This study was conducted in accordance with Good Clinical Practice guidelines and the Declaration of Helsinki. The protocol was approved by the Institution Review Board (IRB) at Scientific Committee of Clinical Oncology, Medical Ethics Review Committee Leiden/Den Haag/Delft [Approval number: G21.200]. As data from routine care were used, a waiver was granted for the requirement of informed consent by IRB.

2.2. Population pharmacokinetics analysis

Using pazopanib concentration versus time after dose data, a POPPK model was developed to describe the PK profiles of the included patients. The study first explored both one- and two-compartment models with first-order oral absorption. Given the known dose-dependent, non-linear absorption characteristics of pazopanib tablets, besides linear absorption, an additional published dual absorption rate (Ka) model, accounting for dose- and time-dependent bioavailability (F1), was evaluated (Yu et al.[20]) by fixing to the published values. In addition, other potential non-linear apparent clearance (CL/F) models were also evaluated. The influence of disease types on the CL/F of pazopanib was also examined. All PK parameters were assumed to follow a log-normal distribution, and inter-individual variability (IIV) was incorporated into different PK parameters as shown in Equation 4.1:

$$P_i = P \cdot e^{(\eta_i, IIV)} \quad (4.1)$$

Where P_i represents the individual PK parameter estimates, P denotes the typical population parameter estimate, and $\eta_i IIV$ represents the random IIV which was assumed to follow a normal distribution with a mean of 0 and a variance of ω^2. The residual error was characterized with a proportional model, or an additive model, or a combined proportional and additive model.

After the structural model was determined, different covariate effects on CL/F and volume of distribution (V/F) were investigated with a stepwise covariate modeling (SCM) algorithm, which is an in-built function of Perl-speaks-NONMEM (PsN, version 5.3.1). The evaluated covariates included tumor type, food effect, age, sex, body weight and BMI. Since pazopanib is a substrate of CYP3A4, concomitant medication of CYP3A4

inhibitors (gastric acid-suppressive agents[21]) was also evaluated. Model selection was based on the change in objective function value (dOFV). The p-values were set as 0.05 (dOFV ≥ 3.84 for 1 more degrees of freedom) for the forward selection and 0.01 (dOFV ≥ 6.64 for 1 more degree of freedom) for the backward elimination process.

Goodness-of-fit (GOF) plots were used to evaluate the fit of the studied models. GOF plots were stratified on tumor types to investigate potential differences between mRCC and STS patients. Bootstrap was used to evaluate model estimation uncertainty. Simulation-based evaluation was carried out with a prediction-corrected visual predictive check (pcVPC).[22]

2.3. Exposure-liver toxicity analysis

A non-parametric Kaplan-Meier plot divided by tumor type was first derived to compare the difference between mRCC and STS. Then, a time-to-first event (TTE) modeling approach was used to explore the hazard of occurrence of CTCAE ≥ 2 liver toxicity between the start of the pazopanib treatment and the last available laboratory investigation records before the end of pazopanib treatment or before the follow-up time ended (censored time was set to 365 days after the initiation of pazopanib treatment). For parametric TTE modeling, the likelihood of the binary event data given the survival function was calculated according to Equation 4.2 and 4.3.

$$S(t) = e^{-cumhaz} \tag{4.2}$$

$$cumhaz = \int_0^t h(t)\, dt \tag{4.3}$$

Where *S(t)* denotes the time course of the probability of survival, *cumhaz* represents the cumulative hazard between the time of follow-up start and the time *t* (the time of the event or the time of censoring) and *h(t)* represents the hazard of an individual subject at the time of the event.

Five basic hazard models were evaluated for the TTE model development, namely weibull, exponential, gompertz, log-logistic and log-Normal models.[23] The hazard model that best fit our data was selected based on the change of OFV and survival-based visual predictive check (sVPC). In addition, a hazard-based VPC (hVPC) adapted from a previously established algorithm and R package[24] was created to assist the evaluation of hazard function.

The established pazopanib POPPK model was used to generate pazopanib exposure over time for all included patients, including $C_{min,ss}$ (the trough concentration on the day of the toxicity event or the day of the censoring), maximum concentration C_{max} (the maximum concentration on the day of the toxicity event or the day of the censoring), area under the curve every 24 hours (AUC24h, on the day of the toxicity event or the day of the censoring). The effect of exposure metrics $C_{min,ss}$, C_{max}, AUC24h (following equations will use EXPOSUREpazo to represent the exposure metrics of pazopanib) was evaluated with a linear and an exponential function (Equation 4.4 and 4.5), where h(t) represents the hazard at the specific time point, h(t)0 represents the base hazard at the start of the pazopanib treatment, EXPOSUREpazo represents the effect of the pazopanib exposure metrics. A more than 3.84 decrease in OFV ($p < 0.05$) after adding EXPOSUREpazo compared with the basic TTE model was considered to suggest a significant effect of exposure metrics on the hazard of liver toxicity occurrence. Finally, a toxicity cut-off target was determined by evaluating different concentrations as a threshold. For this purpose, equation 6 was applied and θ was estimated if the pazopanib concentration was higher than the XX mg/L (or mg*h/L) threshold (Equation 4.6). In addition to EXPOSUREpazo, other covariates including pazopanib dose just before the toxicity event, pazopanib initial dose, age, body weight, sex and tumor type were also evaluated.

$$h(t) = h(t)_0 \cdot (1 + \theta \cdot EXPOSUREpazo) \quad (4.4)$$

$$h(t) = h(t)_0 \cdot e^{(\theta \cdot EXPOSUREpazo)} \quad (4.5)$$

$$If\ EXPOUSREpazo > XX,\ h(t) = h(t)_0 \cdot e^{(\theta \cdot EXPOSUREpazo)} \quad (4.6)$$

2.4. Exposure-tumor size dynamics analysis

Exposure-tumor size dynamics analysis using the sum of longest diameter of target lesions (SLD, in mm) after and during pazopanib as response endpoint was performed. The population was assumed to consist of two sub-populations at the start of treatment: a pazopanib primary sensitive population (SLD_s) and a pazopanib primary resistant population (SLD_r) for which a mixture model was used. The structural model development strategy was: (1) Determine a semi-mechanistic model with apparent growth rate (KG), apparent decay rate (KD) and acquired resistance (λ); (2) Implement a mixture model to identify patients with primary resistance; (3) Investigate the effect of exposure (EXPOSUREpazo, same exposure metrics as in toxicity analysis) on tumor growth and (4) Perform a covariates analysis on the established model. The mRCC and STS population

were first modeled together, and tumor type was used as a covariate. Later, standalone models for both diseases were also developed separately. Due to the sparse tumor size data in the STS population, the baseline tumor size was used as input variable instead of estimating it to improve the stability of the model.

After the mixture model for SLD_s and SLD_r subpopulations was established, pazopanib time-varying exposure metrics derived from the PK model, including the trough concentration of each day of treatment, C_{max}, and AUC24, were added to the model (step (3)). KD was assumed to depend on pazopanib exposure, and linear, exponential, Emax relationship were tested separately to select the best equation.

Finally, the IIVs of parameters were evaluated and parameters were assumed to be log-normally distributed. The combined proportional and additive model was applied to characterize the residual error. The model fit was evaluated by dOFV, GOF plots and pcVPC considering the censoring of data.

2.5. Model-based simulations for treatment optimization

Based on the final pazopanib POPPK model, liver toxicity model and tumor size dynamics model, simulations were performed to optimize the starting dose. Three dose regimens, 800 mg QD, 600 mg QD and 400 mg QD were compared in the simulations. One thousand simulations for each regimen were performed over a follow-up period of 365 days after treatment initiation. Median pazopanib concentration and 90% prediction intervals were plotted to visualize the exposure over time. Additionally, the median probability of developing CTCAE ≥ 2 liver toxicity with 95% confidence intervals were included. Median tumor size over time with 90% prediction intervals was visualized separately for mRCC and STS populations to represent the differences in response between the two tumor types.

Additionally, using the final POPPK model, a shiny application was created based on the "shiny" package (version 1.9.1) and the "mapbayr" package[25] in R (The R Foundation for Statistical Computing) to perform maximum a posterior Bayesian estimation for a random patient with a random measured concentration and to provide dose adjustment recommendations based on the individual parameter and simulations.

2.6. Software and estimation methods

The population PK and PK/PD modeling analyses in this study was performed with NONMEM (version 7.4.4, ICON Development Solutions). First order conditional esti-

mation with interaction (FOCE-I) algorithm was selected as parameter estimation method for POPPK and tumor size modeling. First order (FO) algorithm was selected as likelihood estimation method for toxicity analysis. Data management, data formatting, results visualization and basic statistical analysis were performed with R statistics software (version 4.2.1).

3. RESULTS

3.1. Patient and data

In this model-based analysis, 132 patients were included with a histology diagnosis of mRCC (n = 93) or STS (n = 39) who received pazopanib treatment from 01/2014 to 01/2023 at LUMC. Patients who interrupted the pazopanib for more than 6 months were treated as two different individuals, and therefore the final dataset included 135 patients of which 96 (71%) were mRCC patients. Both mRCC and STS patients were initiated at a median dose of 800 mg (IQR 600–800 mg) QD, and used a median dose of 600 mg (IQR 400–800 mg) QD during the pazopanib treatment as depicted in Table 4.1.

For the pazopanib PK measurements, in total 460 samples were included of which 70% were trough concentrations. The median time after dose was 24 hours with a range of 0.5–166 hours. Median observed pazopanib concentration was 28 mg/L for mRCC and 30 mg/L for STS. Median individual predicted $C_{min,ss}$ was 27 mg/L (IQR 22–35 mg/L) for both tumor types generated by the POPPK model described in Table 4.2. None of the collected concentrations was below the lower limit of quantification.[17] The collected observations over time after dose is shown in Supplemental Figure S4.2.

The laboratory assessment data representing the liver function during pazopanib treatment of all included 135 patients were available for toxicity analysis. 27 out of 135 patients (20%) experienced an CTCAE ≥ 2 elevated ALT, AST or ALP within one year censoring time after treatment initiation. Regarding tumor size, which was expressed as SLD, of the studied population, 24 patients either did not have a traceable baseline SLD or did not undergo a CT scan during pazopanib treatment and were therefore excluded from the cohort for tumor size dynamics analysis. Baseline median SLD of mRCC was 79 (IQR 50–129) mm and STS was 88 (64–148) mm. During the pazopanib treatment, median SLD of mRCC patients was 53 (IQR 33–103) mm, while that of the STS patients was 112 (IQR 61–160) mm. The baseline patient demographics, disease characteristics, dosing information and tumor size data information of the included patients are summarized in Table 4.1.

Table 4.1. Baseline patient demographics, disease characteristics, dosing information and tumor size data information from the included mRCC and STS patients in the analysis

Parameters	Total	mRCC	STS
Patients' characteristics			
Total number of patients (N, %)	135	96 (71%)	39 (29%)
Male/female (% male of total)	85/50 (63%)	69/30 (72%)	16/23 (41%)
Age (years, median [range])	67 [21–89]	69 [48–89]	51 [21–82]
Height (cm, median [range])	173 [147–202]	175 [147–202]	169 [149–196]
Weight (kg, median [range])	79 [45–130]	80 [46–130]	73 [45–124]
BMI (kg/m^2, median [range])	25.4 [17.6–42.5]	25.6 [18.1–42.5]	25.2 [17.6–37.2]
Concomitant therapy			
No gastric acid-suppressive agents	110 (82%)	75 (78%)	35 (90%)
With gastric acid-suppressive agents	25 (18%)	21 (22%)	4 (10%)
Pazopanib dosing			
Pazopanib initial dose per individual (mg, range)	800 (200–800)	800 (200–800)	800 (400–800)
Pazopanib median dose per individual (mg, range)	600 (200–1000)	600 (200–1000)	600 (200–1000)
Pazopanib median treatment days (days, IQR)	120 (63–372)	176 (63–410)	93 (61–192)
Number of individuals with dose reduction occasion (N, %)	66/135 (49%)	50/96 (52%)	16/39 (41%)
Number of individuals with dose increase occasion (N, %)	51/135 (37%)	39/96 (40%)	12/39 (30%)
Pharmacokinetic data			
Total number of observations (N)	460	356	104
Number of trough concentrations (N)	326 (70%)	252 (70%)	74 (71%)
Number of observations per patient (N, median with IQR)	3 (1–23)	3 (1–23)	2 (1–11)
Median overall pazopanib concentration (mg/L, IQR) (n = 460)	29 (2–77)	28 (3–77)	30 (2–75)
Median Trough pazopanib concentration (mg/L, IQR) (n = 324)	27 (22–35)	27 (22–34)	27 (21–39)
Median time after last dose (hr, IQR)	24 (0.5–166)	24 (0.5–166)	24 (2.5–58)
Median time after start of treatment (days, IQR)	120 (63–372)	177 (63–410)	93 (61–193)
Liver toxicity data (N = 135)			
CTCAE GRADE = 1 (N)	55	36	19
CTCAE GRADE = 2 (N)	11	8	3
CTCAE GRADE ≥ 3 (N)	16	13	3
Tumor size (TS) data (N = 111)			
Total number of TS observations (N)	403	322	81
Median number of TS observations per patient (N, IQR)	3 (2–6)	4 (2–6)	2 (1–3)
Median baseline SLD (mm, IQR)	82 (54–134)	79 (50–129)	88 (64–148)
Median SLD during treatment (mm, IQR)	62 (36–111)	53 (33–103)	112 (61–160)

3.2. POPPK model of pazopanib

A one-compartment POPPK model with first order elimination, linear absorption and dose-nonlinearity on bioavailability (F1) was established with the available pazopanib PK data. Due to the limited data in the absorption phase, Ka was fixed to the reported value[26] as this model was also based on a population that from real-world practice.[26] F1 was fixed to 1 and IIV of CL/F, V/F and F1 were estimated resulting in improved model fit. Compared to constant F1, dose-nonlinearity significantly improved the model performance, empirical Bayesian estimates (EBE) distribution and OFV. None of the tested covariates (tumor type, age, body weight, sex) significantly influenced any of the PK parameters. Concomitant of CYP3A4 inhibitors were also not observed to have impact in our cohort. The parameter estimates of the final pazopanib POPPK model are presented in Table 4.2. The relative standard errors (RSEs) were less than 20% for all typical values and slightly higher for IIV of V/F (57%). Bootstrap results indicated a stable estimation, as shown in the last column of Table 4.2.

Table 4.2. POPPK parameter estimates of pazopanib for the final model for mRCC and STS patients, and results of bootstrap

Parameters	Estimates (RSE) [Shrinkage]	Bootstrap results (median + 95% CI)
CL/F (L/h)	0.497 (7%)	0.490 (0.40–0.57)
V/F (L)	46.1 (19%)	44.6 (32.6–63.0)
Ka (h)	0.976 FIX[24]	0.976 FIX[24]
$F1 = TVF_1 * (200/DOSE)^{EXP}$		
TVF_1	1 FIX	1 FIX
EXP	0.42 (12%)	0.43 (0.32–0.57)
IIV_V/F (CV%)	76.5% (16%) [51%]	72.1% (45.5–92.7%)
IIV_F1(CV%)	34.2% (9%) [15%]	34.0% (27.9–40.0%)
Proportional error (CV%)	24% (10%)	24% (16–29%)
Additive error (mg/L)	4.71 (20%)	4.60 (1.15–7.48)

CL/F, apparent clearance; V/F, volume of distribution; Ka, absorption rate constant; F1, bioavailability; IIV_CL, inter individual variability of clearance; IIV_V, inter individual variability of volume of distribution; IIV_F1, inter individual variability of bioavailability.

The GOF plots of the final pazopanib PK model demonstrated an adequate description of observations by both individual predictions (IPRED) and population predictions (PRED), as shown in Supplemental Figure S4.3. The conditional weighted residual errors (CWRES) were randomly distributed around zero without obvious trends over population predictions and TAD. pcVPC of 1000 simulations indicated a well description of the model to the data as shown in Supplemental Figure S4.4 (a). Dose linearity was also depicted in Supplemental Figure S4.4 (b).

3.3. Exposure-liver toxicity analysis

The raw data visualization of percentage change of liver enzyme (yellow line) over time and pazopanib predicted $C_{min,ss}$ over time (dashed black line) after pazopanib treatment initiation of each individual are provided in Supplemental Figure S4.5. The non-parametric Kaplan-Meier analysis of observed events of CTCAE ≥2 liver toxicity and censored data with confidence interval is depicted in Figure S4.6, showing that there is no significant difference in developing a liver toxicity event between mRCC and STS patients while higher $C_{min,ss}$ (≥ 34 mg/L) significantly difference from lower $C_{min,ss}$ group (< 34 mg/L). A gompertz model was selected as the base model with a significant lower OFV (dOFV > 20) than the other models and described the data well.

Covariates including pazopanib dose on the day before the toxicity event, pazopanib initial dose, different exposure metrics, age, body weight, sex and tumor type, were tested on the base hazard model. Due to correlations between dose and exposure metrics, only a first round of covariate selection was performed, and the most significant covariate was selected. $C_{min,ss}$ had a largest dOFV of 8.03 and was selected as covariate. The hazard of developing liver toxicity did not differ between mRCC and STS as depicted in Supplemental Figure S4.5. A $C_{min,ss}$ of ≥ 34 mg/L was identified as the liver toxicity threshold that resulted in a significant increase in hazard (i.e. 3.35-fold hazard increase ($p < 0.01$)) compared to $C_{min,ss}$ < 34 mg/L. Details of the hazard ratio fold changes are depicted in Supplemental Table S4.1 and Supplemental Figure S4.7, where it could be observed that the hazard would be increased and maintained at high coefficient when $C_{min,ss}$ ≥ 34 mg/L. The parameter estimates of the final toxicity model was provided in Table 4.3. The SHAPE parameter indicated the general trend of the hazard where in our analysis SHAPE = -0.012 per day indicated the hazard decreased from the baseline over time. The survival-based VPC of final toxicity model, as shown in Figure 4.1, indicates a significantly lower CTCAE ≥2 liver toxicity-free survival when $C_{min,ss}$ > 34 mg/L. Hazard-based VPC, which was provided in Supplemental Figure S4.8, indicated well alignments between model-predicted hazard and the true hazard.

Table 4.3. Parameter estimates of final TTE model with a Gompertz distribution

Parameters	Estimates (RSE)	Bootstrap results (median + 95% CI)
LAMDA (1/Day)	0.0021 (33%)	0.0020 (0.0010, 0.0034)
SHAPE (1/Day)	-0.012 (28%)	-0.012 (-0.021, -0.007)
$C_{min,ss}$ COEFFICIENT (coef)*&	1.21 (32%)&	1.30 (0.93, 2.07)

* $If\ C_{min,ss} > 34\ mg/\mathrm{L}$, $\mathrm{h}(t) = LAMDA * e^{(SHAPE*TIME)} * e^{(coef)}$ $[Time\ unit = Day]$.
& The fold change is e(coef) = 3.35.

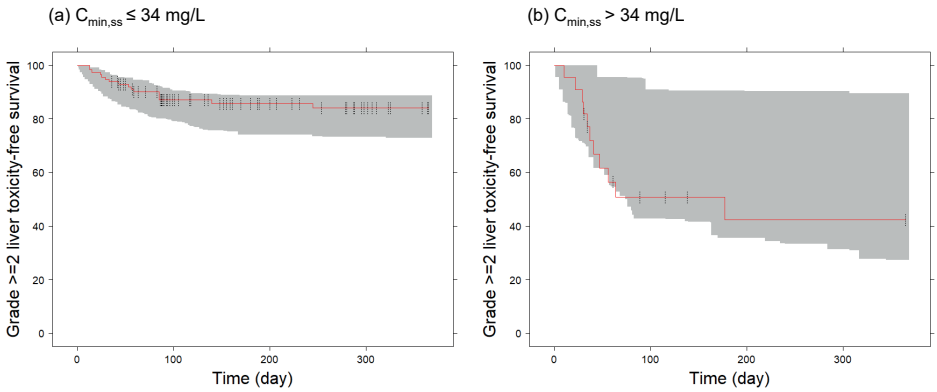

Figure 4.1. Survival-based visual predictive check Kaplan-Meier plots of the Grade ≥ 2 liver toxicity free probability over one year censoring time stratified by $C_{min,ss}$ threshold of 34 mg/L derived from the final liver toxicity model. The solid red lines represent the Kaplan–Meier curve of the observed data and the grey shaded areas represent the 95% prediction interval. The vertical lines represent censored observations.

3.4. Exposure-tumor size dynamics analysis

The visualization of collected SLD data was depicted in Supplemental Figure S4.9. For the tumor size dynamics model, the model structure was the same for both tumor types and is shown in Figure 4.2 and Equations 4.7–4.8. The tumor size modeling results, as depicted in Table 4.4, showed that the tumor growth model accounting for the presence of different sub-populations that have primary resistance and/or acquired resistance could adequately describe the collected SLD data. The introduction of a sub-population with primary resistance by using a mixture model, improved the model fit significantly (27% and 13% for mRCC and STS, dOFV > 3.84), as well as the distribution of ETA on decay rate (KD) with a shift towards a more normal distribution and reduced skewness. For tumor growth rate estimates (KG), first-order apparent growth rate (day-1) was estimated to be 0.0005 for mRCC and 0.0086 for STS. For the KD, a linear decay rate was estimated (0.004 day-1 for mRCC and 0.008 day-1 for STS) while neither exposure nor dose dependency was identified as significant covariate for any of the tumor types. Acquired resistance rate λ (day-1) was described by an exponential function with time dependency (0.008 for mRCC and 0.0003 for STS). RSE for all estimates were ≤ 30% except resistance rate of STS (59%). Detailed diagnostic plots of the final tumor size dynamic model are shown in Figure 4.3 and a VPC based on 1000 simulations and considering drop-out is presented in Supplemental Figure S4.10.

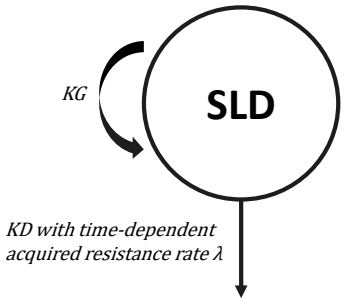

For primary sensitive population (SLD_s):

$$\frac{dSLD\_s}{dt} = KG * SLD\_s - KD * e^{-\lambda t} * SLD\_s \quad (4.7)$$

For primary resistant population (SLD_r):

$$\frac{dSLD\_r}{dt} = KG * SLD\_r \quad (4.8)$$

Figure 4.2. Final tumor size model structure based on sum of longest diameters (SLD) for both mRCC and STS (KG: growth rate; KD: decay rate; λ: acquired resistance rate). Primary sensitive population (SLD_s) and primary resistant population (SLD_r) were distinguished by implementing a mixture model in NONMEM. SLD_r was assumed to have no drug-induced decay and therefore KD was fixed to 0.

Table 4.4. Parameter estimates of tumor size dynamics model

	mRCC		STS	
Tumor type	Estimate (RSE%)	Bootstrap (median + 95% CI)	Estimate (RSE%)	Bootstrap (median + 95% CI)
Growth rate KG (day-1)	0.0005 (31)	0.0005 (0.0002–0.001)	0.0086 (22)	0.0086 (0.0085–0.0087)
Decay rate KD (day-1)	0.004 (15)	0.004 (0.003–0.006)	0.008 (24)	0.0078 (0.0078–0.008)
Acquired resistant rate λ (day-1)	0.008 (16)	0.008 (0.006–0.012)	0.0003 (59)	0.0003 (0.0002–0.0004)
Subpopulation of primary resistance (%)	27% (12)	26% (8–50%)	13.4% (8)	14% (10–23%)
Random effects CV% [shrinkage%]				
IIV_KG	130% (18) [27]	125% (77–167%)	0 FIX	/
1IIV_KD	54% (20) [27]	46% (30–64%)	13% (33) [30]	12% (6.7–17.8%)
Residual error (RSE%)				
Prop.err (%)	13.8% (3)	14% (11–17%)	16.6% (18)	17% (0.16–0.17)
Add.err (mm)	1.24 (33)	1.12 (1–1.63)	8.1 (71)	8.2 (8–8.2)

3.5. Model-based simulations for dose optimization

Model-based simulations of the final models on pazopanib exposure over time, CTCAE ≥ 2 liver toxicity probability over time and tumor size dynamics over time after pazopanib treatment were performed to compare different pazopanib initial dose regimens. As depicted in Figure 4.4, the 800 mg and the 600 mg QD starting dose are anticipated to lead to adequate efficacy, as $C_{min,ss}$ remains above the target threshold of 20.5 mg/L in 76% of the simulated individuals while the 800 mg starting dose significantly increased the hazard of developing a liver toxicity event. For both mRCC and STS, no additional exposure or dose dependency was observed (right panel).

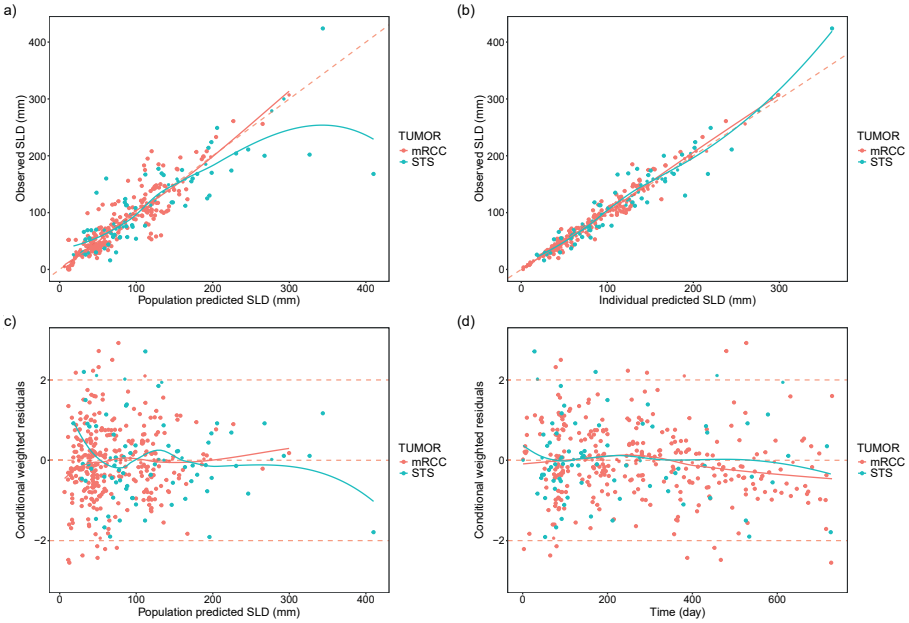

Figure 4.3. Goodness-of-fit plots of final TS dynamics model. **(a)** population predicted SLD versus observed SLD; **(b)** Individual predicted SLD versus observed SLD; **(c)** population predicted SLD versus conditional weighted residual errors; **(d)** Time after treatment start versus conditional weighted residual errors.

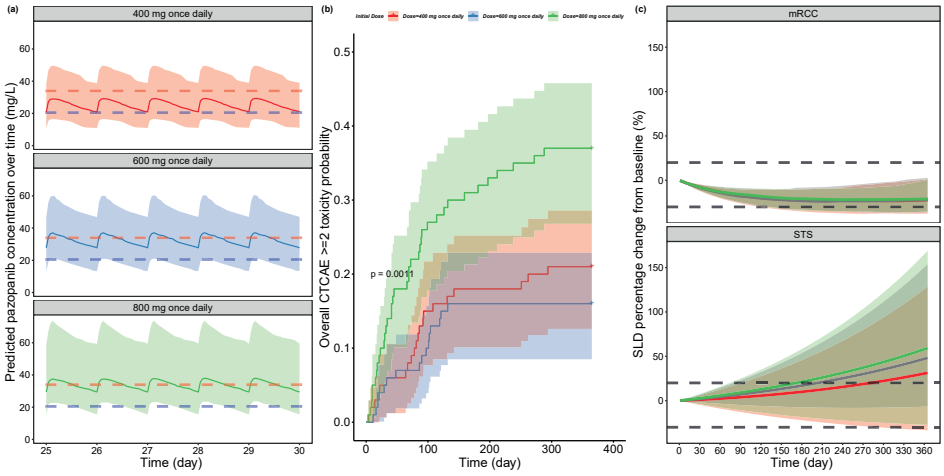

Figure 4.4. Model-based simulations of approved 800 mg once daily starting dose (green) and reduced starting doses (600 mg once daily (blue), 400 mg once daily (red)) with the final pazopanib POPPK model, final liver toxicity model and final tumor size dynamics model. **(a)** Pazopanib exposure over time of three different dosing regimens, where solid lines represent the median exposure filled with an 90% prediction interval. Blue dashed lines represent the 20.5 mg/L efficacy threshold and red dashed lines represents the 34 mg/L toxicity threshold. **(b)** Overall CTCAE ≥ 2 liver toxicity probability over time after pazopanib treatment of three dosing regimens (where solid lines represent the median survival curve filled with a 95% confidence interval). **(c)** SLD percentage change from baseline over time after pazopanib treatment of three dosing regimens, where solid lines represent the median percentage change of SLD from baseline filled with a 90% prediction interval, for mRCC and STS patients. The grey dashed lines represent the RECIST1.1 criteria of stable disease (SLD shrinkage from -30% to 20%).

Tumor sizes highly overlapped for both regimens, regardless of the tumor type. A shiny application was developed in which a randomly collected pazopanib PK sample can be the input, and it will provide the current predicted $C_{min,ss}$ and the $C_{min,ss}$ values for alternative regimens as a reference (Supplemental Figure S4.11).

4. DISCUSSION

In this study, we performed a comprehensive evaluation of the pazopanib POPPK, exposure-liver toxicity relationship and exposure-tumor size dynamics of real-world patients with mRCC and STS treated with pazopanib. A one-compartment POPPK model with dose-nonlinearity on F1 described the data well. In the exposure-liver toxicity analysis, $C_{min,ss}$ was identified as significant covariate and a $C_{min,ss}$ threshold > 34 mg/L indicated a 3.35-fold higher hazard of CTCAE Grade ≥ 2 liver toxicity compared to $C_{min,ss}$ ≤ 34 mg/L. Exposure-tumor size dynamic models incorporating tumor heterogeneity were established for both tumor types, separately. No additional pazopanib dose or exposure effect on tumor growth was observed in our cohort with TDM trough samples generally above 20.5 mg/L which suggest that the current $C_{min,ss}$ target was adequate for both mRCC and STS.

There is ample evidence suggesting that the approved 800 mg QD pazopanib fixed dose is not the optimal initial dose. The approved dose was established using the maximum tolerated dose (MTD) paradigm where no dose limiting toxicities were identified and only one dose level of 800 mg QD was evaluated in the registration study.[27] According to the FDA registration file,[28] the FDA reviewers combined all available patients from the clinical trials[28] and divided the $C_{min,ss}$ into quantiles for a survival analysis. The survival curves of patients with different trough concentration-quartile groups overlapped at several points, suggesting the absence of exposure-response within the exposure range upon the 800 mg QD dosing regimen. A logistic regression analysis was performed with registration trial toxicity data[29] and found that the probability of Grade 3+ ALT increased with increased pazopanib exposure. This reflects a limitation of the MTD paradigm, which prioritizes a highest tolerated dose rather than a dose optimized for long-term tolerability and efficacy. The FDA's recent initiative, project OPTIMUS,[30] emphasized the importance to achieve an optimal dose by considering multiple factors like nonclinical data, PK/PD, biomarker, prior knowledge, modeling & simulation tools, rather than only evaluating the MTD in registration study. In clinical practice, the dose reduction rate (DRR) and related outcomes are reported in several

published studies. The DRR ranged from around 40%[31] to 60%[11, 32] in different studies. A statistically significant longer PFS (median 18.2 [95% CI 14.8–21.6] versus 8.2 months [95% CI 6.2–10.2]) and OS (median 30.7 [95% CI 23.6–37.9] versus 19.1 months [95% CI 14.7–23.4]) in patients who underwent dose reductions compared to patients who maintained the starting dose ($p < 0.0001$), was reported in a retrospective study with 179 mRCC patients that almost exclusively received pazopanib as first-line treatment.[33] Moreover, a food effect study[34] identified that the intake of 600 mg pazopanib with breakfast resulted in a bioequivalent exposure established with 800 mg fasted and was preferred over a standard pazopanib dose without food due to less toxicity.

Previously, several pazopanib POPPK models have been published based on different populations. The first pazopanib POPPK model was retrieved from the FDA registration file,[28] where a one compartment model with dose-dependent KA was established (the FDA model[28]). A more complex two-compartment disposition model with dual absorption, time-dependent and dose-dependent F1 was reported by Yu et al. (Yu model[20]) using three clinical trials datasets.[20] Later on, a one compartment model with a simple absorption model, based on real-world data, was reported by Ozbey et al26 (the Ozbey model[26]). The typical value of Ka (0.976 h-1) from the Ozbey model26 was adopted by our study. Different absorption models, with time-dependent or dose-dependent KA and/or F1, were tested including the complex model from the Yu model.[20] A simplified dose-nonlinearity model, which is a power function, on F1 could describe our data better than the original complex one due to sparse information on this parameter in our dataset. The estimated CL/F in our analysis is 0.497 L/h, which is the same as reported in the Ozbey model[26] and lower than the estimate reported by the FDA model (0.997 L/h). The V/F estimated from our study is 46 L, which is the same as the FDA model (45 L) and higher than the Ozbey model (22 L). To sum up, it seems that the broad range of real-world patients could have lower pazopanib clearance on average (and therefore higher concentrations) than the clinical trial population.

Dinduced liver toxicity (DILI) is a daily challenge in routine clinical practice.[35] Pazopanib is known for the frequent occurrence of DILI of around 60% patients who develop moderate liver toxicity which requires dose reduction or dose interruption.[33] Furthermore, 12% of all patients will develop severe liver toxicity which requires dose interruption until remission of symptoms.[36] However, there is no CTCAE ≥ 2 liver toxicity target was proposed so far. Previously, a threshold of $C_{min,ss} \leq 50.3$ mg/L for overall Grade ≥ 3 toxicity was proposed.[13] Another similar threshold of $C_{min,ss} \leq 46$ mg/L was proposed also for overall severe toxicity.[12, 37] A real-world study focusing on liver toxicity tried to

investigate the exposure difference between patients that had or did not have CTCAE ≥ 2 liver toxicity.[38] However, pazopanib exposure was comparable in patients with or without liver toxicity (27.7 mg/L versus 28.1 mg/L) and the calculation of $C_{min,ss}$ was based on non-compartmental equations rather than based on a modeling approach, which may introduce bias of achieving the "true" $C_{min,ss}$ at the time of the toxicity event.[38] In addition, non-parametric logistic regression was applied in previous research where the time-varying exposure was not taken into consideration.[38] In the current analysis, different exposure metrics were generated by a well-defined POPPK model and parametric TTE modeling approach, which provided an opportunity to simulate different scenarios. A CTCAE ≥ 2 liver toxicity specific threshold of $C_{min,ss}$ ≤ 34 mg/L was determined based on the evaluation of several thresholds, aiming to improve continuation of long-term treatment.

Previously, the tumor growth behavior of RCC was investigated by several studies, at both pre-clinical and clinical stage, where linear,[39, 40] exponential,[41] quadratic[42] and logistic[43] models were reported using different datasets. These previously reported growth models were tested in this study. However, the prior knowledge of tumor growth behavior for STS was limited and only data on an individual-level was available.[44] In addition, no study from real-world evidence was reported for mRCC or STS.[40, 42, 43] In the pre-clinical phase,[43] a logistic tumor growth model with an angiogenesis process was implemented where first order exposure effect (pazopanib area under the curve) was added into the model even though it was unclear whether or how it impacted the model performance. In clinical development,[42] a quadratic growth term and a mixture model was implemented to allocate patients in Group 1 or Group 2. Group 1 accounted for 93% of the population with subsequent tumor regrowth. Group 2 accounted for 7% of the population, which showed tumor shrinkage without subsequent tumor regrowth. Pazopanib increased the tumor shrinkage rate in a dose-dependent manner in Group 1 patients. Pazopanib 800 mg increased the tumor shrinkage rate by 267% (95% CI 215–319%) compared with placebo. In contrast, the tumor shrinkage rate in Group 2 patients was independent of treatment (pazopanib or placebo) and had high IIV and high residual variability. Different from previously published tumor size models for pazopanib, neither dose nor exposure effect was observed to be relevant to tumor shrinkage in our analysis, where the median $C_{min,ss}$ was 26.6 mg/L with IQR 20.6–31.1 mg/L. This indicates that the 20.5 mg/L efficacy threshold is also applicable for STS patients. Similar evidence could be retrieved from the FDA clinical pharmacology report of pazopanib.[28] The FDA reviewers combined all available patients from the trials28 and

divided the $C_{min,ss}$ into quantiles for survival analysis. The survival curves of patients with different trough concentration-quartile groups overlapped at several points, indicating the absence of exposure-response with the 800 mg QD dosing regimen.

The ultimate goal of this comprehensive model-based analysis is to employ the results for pazopanib MIPD in routine practice. MIPD has been widely used to optimize the dosing schedule of antibiotics to ensure drug exposure over minimal inhibitory concentrations (MIC)[45] while there is still only limited application in oncology. Previously, case studies have proved that MIPD can improve the initial dose of imatinib[46] and reduce vincristine-induced peripheral neuropathy in pediatric patients.[47] Recently, Le Loudec et al. developed "mapbayr" R package,[25] which aims to perform maximum a posteriori Bayesian estimation in R from any POPPK model. Based on the pazopanib MIPD shiny example developed by Le Loudec et al., we replaced the model with our POPPK model that could be more representative for real-world population and introduced the threshold of 20.5 mg/L ≤ $C_{min,ss}$ ≤ 34 mg/L for both cancer population. The shiny application can generate the dose adjustment recommendation from extrapolating randomly taken samples to trough levels. The details of our updated pazopanib MIPD shiny application can be found at https://github.com/tanzy1995/pazopanib-MIPD. There are commercial MIPD tools available that could incorporate PK models as the one provided in our manuscript. However, the application of MIPD tools such as the shiny interface provided in this manuscript in routine clinical practice faces significant challenges. These challenges include the requirement of a lot of (legal) documentation, validation and testing is required for every change that is made to the tool even it is used solely in an ISO15189 laboratory environment. These tools in general, while promising for improving individualized dosing, currently occupy a regulatory oversight where a clear framework are formally required to label them as medical devices.[48] This ambiguity complicates their widespread adoption, especially considering the potential risk of using these tools to prescribe off-label dose, which could lead to safety concerns.[48, 49] Additionally, the integration of MIPD into clinical workflows requires overcoming operational barriers, such as the need for real-time data input, model validation, and proper healthcare professional education.[49, 50] Collaborative efforts among diverse stakeholders for MIPD tools regulation (clear regulation pathway), model validation, education and implementation are warranted.[48-50]

The present study has some limitations. First, due to the rare nature of STS, only a limited number of data could be retrieved for the tumor size data of STS patients. In addition, no prior knowledge on the tumor growth behavior, killing effect and resistance could

be found for STS. In that case, the KG rate, KD rate and resistance rate of STS were all interpreted as "apparent" constant rate rather than a "real" constant rate. In our analysis, we used baseline tumor size as regressor rather than estimating it to have stable estimation. However, this study is the first that investigated the relationships between PK, toxicity and tumor size dynamics of pazopanib not only in mRCC but also STS in real-world setting. Secondly, due to the fact that the data in our analysis were collected from real-world practice which included TDM, most of the included patients were well managed according to the current pazopanib TDM guidelines[51-53] and therefore the median predicted $C_{min,ss}$ was 26.6 mg/L with IQR 20.6–31 mg/L, which was beyond the established efficacy threshold. Potential bias could be introduced when the pazopanib exposure or dose effect on tumor size dynamics was investigated with pazopanib $C_{min,ss}$ < 20.5 mg/L being evaluated in only 16 out of 111 patients (14%). Finally, only moderate liver toxicity was evaluated in the toxicity analysis due to the limited number of severe events that occurred in our cohort. Therefore, further analysis with more extensive data is warranted to validate the current liver toxicity threshold and to explore the correlation between pazopanib dose/exposure and severe (CTCAE Grade ≥ 3) liver toxicity. Also, other frequent toxicities like diarrhea, increased MAP, stomatitis should also be considered in future studies.

5. CONCLUSION

The pazopanib exposure-liver toxicity model indicates that a $C_{min,ss}$ > 34 mg/L significantly increases the risk of developing CTCAE ≥ 2 liver toxicity for mRCC and STS. In contrast, no clear effect of exposure was observed in the exposure-tumor size dynamics model for both tumor types within our cohort with a median $C_{min,ss}$ of 26.6 mg/L and IQR 20.6–31.1 mg/L. A decreased pazopanib initial dose of 600 mg QD fasted, followed by routine MIPD practice once 2–3 months aiming at a $C_{min,ss}$ target of 20–34 mg/L with the developed POPPK model could potentially improve the balance between efficacy and treatment toxicity.

STATEMENTS AND DECLARATIONS

Conflict of interest

No disclosures are applicable for this work. None of the other authors have any conflicts to declare.

Ethics approval

This study was conducted in accordance with Good Clinical Practice guidelines and the Declaration of Helsinki. The protocol was approved by the Institution Review Board (IRB) at Scientific Committee of the department of Medical Oncology, Medical Ethics Review Committee Leiden/Den Haag/Delft. As retrospective data from routine clinical care were used, a waiver was granted for the requirement of informed consent by the IRB.

Consent to participate/ consent for publication

As retrospective data from routine clinical care were used, a waiver was granted for the requirement of informed consent by the IRB.

Acknowledgement

The authors would like to acknowledge Max Kramer and Mike Volwater for their contribution to this work.

REFERENCES

1. Miyamoto, S.; Kakutani, S.; Sato, Y.; Hanashi, A.; Kinoshita, Y.; Ishikawa, A. Drug review: Pazopanib. Jpn J Clin Oncol 2018, 48 (6), 503-513. DOI: 10.1093/jjco/hyy053
2. Sternberg, C. N.; Hawkins, R. E.; Wagstaff, J.; Salman, P.; Mardiak, J.; Barrios, C. H.; Zarba, J. J.; Gladkov, O. A.; Lee, E.; Szczylik, C.; et al. A randomised, double-blind phase III study of pazopanib in patients with advanced and/or metastatic renal cell carcinoma: final overall survival results and safety update. European journal of cancer (Oxford, England: 1990) 2013, 49 (6), 1287-1296. DOI: 10.1016/j.ejca.2012.12.010
3. Escudier, B.; Porta, C.; Schmidinger, M.; Rioux-Leclercq, N.; Bex, A.; Khoo, V.; Grünwald, V.; Gillessen, S.; Horwich, A. Renal cell carcinoma: ESMO Clinical Practice Guidelines for diagnosis, treatment and follow-up†. Ann Oncol 2019, 30 (5), 706-720. DOI: 10.1093/annonc/mdz056
4. Ljungberg, B.; Albiges, L.; Abu-Ghanem, Y.; Bensalah, K.; Dabestani, S.; Fernández-Pello, S.; Giles, R. H.; Hofmann, F.; Hora, M.; Kuczyk, M. A.; et al. European Association of Urology Guidelines on Renal Cell Carcinoma: The 2019 Update. Eur Urol 2019, 75 (5), 799-810. DOI: 10.1016/j.eururo.2019.02.011
5. van der Graaf, W. T.; Blay, J. Y.; Chawla, S. P.; Kim, D. W.; Bui-Nguyen, B.; Casali, P. G.; Schöffski, P.; Aglietta, M.; Staddon, A. P.; Beppu, Y.; et al. Pazopanib for metastatic soft-tissue sarcoma (PALETTE): a randomised, double-blind, placebo-controlled phase 3 trial. Lancet (London, England) 2012, 379 (9829), 1879-1886. DOI: 10.1016/s0140-6736(12)60651-5
6. Nguyen, D. T.; Shayahi, S. Pazopanib: approval for soft-tissue sarcoma. Journal of the advanced practitioner in oncology 2013, 4 (1), 53-57. DOI: 10.6004/jadpro.2013.4.1.6
7. Suttle, A. B.; Ball, H. A.; Molimard, M.; Hutson, T. E.; Carpenter, C.; Rajagopalan, D.; Lin, Y.; Swann, S.; Amado, R.; Pandite, L. Relationships between pazopanib exposure and clinical safety and efficacy in patients with advanced renal cell carcinoma. Br J Cancer 2014, 111 (10), 1909-1916. DOI: 10.1038/bjc.2014.503
8. Mueller-Schoell, A.; Groenland, S. L.; Scherf-Clavel, O.; van Dyk, M.; Huisinga, W.; Michelet, R.; Jaehde, U.; Steeghs, N.; Huitema, A. D. R.; Kloft, C. Therapeutic drug monitoring of oral targeted antineoplastic drugs. Eur J Clin Pharmacol 2020. DOI: 10.1007/s00228-020-03014-8
9. Sternberg, C. N.; Davis, I. D.; Mardiak, J.; Szczylik, C.; Lee, E.; Wagstaff, J.; Barrios, C. H.; Salman, P.; Gladkov, O. A.; Kavina, A.; et al. Pazopanib in locally advanced or metastatic renal cell carcinoma: results of a randomized phase III trial. J Clin Oncol 2010, 28 (6), 1061-1068. DOI: 10.1200/jco.2009.23.9764

10. Motzer, R. J.; Hutson, T. E.; Cella, D.; Reeves, J.; Hawkins, R.; Guo, J.; Nathan, P.; Staehler, M.; de Souza, P.; Merchan, J. R.; et al. Pazopanib versus sunitinib in metastatic renal-cell carcinoma. The New England journal of medicine 2013, 369 (8), 722-731. DOI: 10.1056/NEJMoa1303989
11. Gaillard, V.; Lhuillier, A.; Bigot, C.; Pierard, L.; Trensz, P.; Burgy, M.; Schuster, C.; Malouf, G.; Fritsch, A.; Lang, H.; et al. Impact of the app-based and nurse-led supportive care program AKO@dom on dose intensity of oral-targeted therapies in patients with metastatic renal cell cancer: a multicentric observational retrospective study. Supportive care in cancer: official journal of the Multinational Association of Supportive Care in Cancer 2022, 30 (8), 6583-6591. DOI: 10.1007/s00520-022-07088-1
12. Lin, Y.; Ball, H. A.; Suttle, B.; Mehmud, F.; Amado, R. G.; Hutson, T. E.; Pandite, L. N. Relationship between plasma pazopanib concentration and incidence of adverse events in renal cell carcinoma. Journal of Clinical Oncology 2011, 29 (7_suppl), 345-345. DOI: 10.1200/jco.2011.29.7_suppl.345.
13. Noda, S.; Yoshida, T.; Hira, D.; Murai, R.; Tomita, K.; Tsuru, T.; Kageyama, S.; Kawauchi, A.; Ikeda, Y.; Morita, S. Y.; et al. Exploratory Investigation of Target Pazopanib Concentration Range for Patients With Renal Cell Carcinoma. Clinical genitourinary cancer 2019, 17 (2), e306-e313. DOI: 10.1016/j.clgc.2018.12.001
14. Minichmayr, I. K.; Dreesen, E.; Centanni, M.; Wang, Z.; Hoffert, Y.; Friberg, L. E.; Wicha, S. G. Model-informed precision dosing: State of the art and future perspectives. Advanced Drug Delivery Reviews 2024, 215, 115421. DOI: https://doi.org/10.1016/j.addr.2024.115421.
15. Escudero-Ortiz, V.; Domínguez-Leñero, V.; Catalán-Latorre, A.; Rebollo-Liceaga, J.; Sureda, M. Relevance of Therapeutic Drug Monitoring of Tyrosine Kinase Inhibitors in Routine Clinical Practice: A Pilot Study. In Pharmaceutics, 2022; Vol. 14.
16. Gotta, V.; Widmer, N.; Decosterd, L. A.; Chalandon, Y.; Heim, D.; Gregor, M.; Benz, R.; Leoncini-Franscini, L.; Baerlocher, G. M.; Duchosal, M. A.; et al. Clinical usefulness of therapeutic concentration monitoring for imatinib dosage individualization: results from a randomized controlled trial. Cancer chemotherapy and pharmacology 2014, 74 (6), 1307-1319. DOI: 10.1007/s00280-014-2599-1.
17. van Erp, N. P.; de Wit, D.; Guchelaar, H. J.; Gelderblom, H.; Hessing, T. J.; Hartigh, J. A validated assay for the simultaneous quantification of six tyrosine kinase inhibitors and two active metabolites in human serum using liquid chromatography coupled with tandem mass spectrometry. Journal of chromatography. B, Analytical technologies in the biomedical and life sciences 2013, 937, 33-43. DOI: 10.1016/j.jchromb.2013.08.013
18. Common Terminology Criteria for Adverse Events (CTCAE) v5.0. 2017. https://ctep.cancer.gov/protocoldevelopment/electronic_applications/ctc.htm#ctc_50 (accessed 2017 27/11/2017).
19. Schwartz, L. H.; Litière, S.; de Vries, E.; Ford, R.; Gwyther, S.; Mandrekar, S.; Shankar, L.; Bogaerts, J.; Chen, A.; Dancey, J.; et al. RECIST 1.1-Update and clarification: From the RECIST committee. European journal of cancer (Oxford, England : 1990) 2016, 62, 132-137. DOI: 10.1016/j.ejca.2016.03.081
20. Yu, H.; van Erp, N.; Bins, S.; Mathijssen, R. H.; Schellens, J. H.; Beijnen, J. H.; Steeghs, N.; Huitema, A. D. Development of a Pharmacokinetic Model to Describe the Complex Pharmacokinetics of Pazopanib in Cancer Patients. Clinical pharmacokinetics 2017, 56 (3), 293-303. DOI: 10.1007/s40262-016-0443-y From NLM.
21. Mir, O.; Touati, N.; Lia, M.; Litière, S.; Le Cesne, A.; Sleijfer, S.; Blay, J. Y.; Leahy, M.; Young, R.; Mathijssen, R. H. J.; et al. Impact of Concomitant Administration of Gastric Acid-Suppressive Agents and Pazopanib on Outcomes in Soft-Tissue Sarcoma Patients Treated within the EORTC 62043/62072 Trials. Clin Cancer Res 2019, 25 (5), 1479-1485. DOI: 10.1158/1078-0432.Ccr-18-2748
22. Bergstrand, M.; Hooker, A. C.; Wallin, J. E.; Karlsson, M. O. Prediction-corrected visual predictive checks for diagnosing nonlinear mixed-effects models. The AAPS journal 2011, 13 (2), 143-151. DOI: 10.1208/s12248-011-9255-z
23. Van Wijk, R. C.; Simonsson, U. S. H. Finding the right hazard function for time-to-event modeling: A tutorial and Shiny application. CPT: pharmacometrics & systems pharmacology 2022, 11 (8), 991-1001. DOI: 10.1002/psp4.12797
24. Huh, Y.; Hutmacher, M. M. Application of a hazard-based visual predictive check to evaluate parametric hazard models. Journal of pharmacokinetics and pharmacodynamics 2016, 43 (1), 57-71. DOI: 10.1007/s10928-015-9454-9
25. Le Louedec, F.; Puisset, F.; Thomas, F.; Chatelut, É.; White-Koning, M. Easy and reliable maximum a posteriori Bayesian estimation of pharmacokinetic parameters with the open-source R package mapbayr. CPT: pharmacometrics & systems pharmacology 2021, 10 (10), 1208-1220. DOI: https://doi.org/10.1002/psp4.12689.

26. Ozbey, A. C.; Combarel, D.; Poinsignon, V.; Lovera, C.; Saada, E.; Mir, O.; Paci, A. Population Pharmacokinetic Analysis of Pazopanib in Patients and Determination of Target AUC. Pharmaceuticals (Basel, Switzerland) 2021, 14 (9). DOI: 10.3390/ph14090927
27. Hurwitz, H. I.; Dowlati, A.; Saini, S.; Savage, S.; Suttle, A. B.; Gibson, D. M.; Hodge, J. P.; Merkle, E. M.; Pandite, L. Phase I trial of pazopanib in patients with advanced cancer. Clinical cancer research: an official journal of the American Association for Cancer Research 2009, 15 (12), 4220-4227. DOI: 10.1158/1078-0432.Ccr-08-2740
28. VOTRIENT (pazopanib) tablets CLINICAL PHARMACOLOGY AND BIPHARMACEUTICS REVIEW.
29. Motzer, R. J.; Hutson, T. E.; Cella, D.; Reeves, J.; Hawkins, R.; Guo, J.; Nathan, P.; Staehler, M.; de Souza, P.; Merchan, J. R.; et al. Pazopanib versus Sunitinib in Metastatic Renal-Cell Carcinoma. New England Journal of Medicine 2013, 369 (8), 722-731. DOI: 10.1056/NEJMoa1303989.
30. US Food and Drug Administration. Optimizing the Dosage of Human Prescription Drugs and Biological Products for the Treatment of Oncologic Diseases, Guidance for Industry. 2024.
31. Shah, A. Y.; Kotecha, R. R.; Lemke, E. A.; Chandramohan, A.; Chaim, J. L.; Msaouel, P.; Xiao, L.; Gao, J.; Campbell, M. T.; Zurita, A. J.; et al. Outcomes of patients with metastatic clear-cell renal cell carcinoma treated with second-line VEGFR-TKI after first-line immune checkpoint inhibitors. European journal of cancer (Oxford, England: 1990) 2019, 114, 67-75. DOI: 10.1016/j.ejca.2019.04.003
32. Johnston, H.; Deal, A. M.; Morgan, K. P.; Patel, B.; Milowsky, M. I.; Rose, T. L. Dose Intensity in Real-World Patients With Metastatic Renal Cell Carcinoma Taking Vascular Endothelial Growth Factor Receptor Tyrosine Kinase Inhibitors. Clinical genitourinary cancer 2023, 21 (3), 357-365. DOI: 10.1016/j.clgc.2023.02.007
33. Corianò, M.; Giannarelli, D.; Scartabellati, G.; De Giorgi, U.; Brighi, N.; Fornarini, G.; Tommasi, C.; Giudice, G. C.; Rebuzzi, S. E.; Puglisi, S.; et al. Tailoring treatment with cabozantinib or pazopanib in patients with metastatic renal cell carcinoma: does it affect outcome? Expert review of anticancer therapy 2023, 23 (5), 545-554. DOI: 10.1080/14737140.2023.2200168
34. Lubberman, F. J. E.; Gelderblom, H.; Hamberg, P.; Vervenne, W. L.; Mulder, S. F.; Jansman, F. G. A.; Colbers, A.; van der Graaf, W. T. A.; Burger, D. M.; Luelmo, S.; et al. The Effect of Using Pazopanib With Food vs. Fasted on Pharmacokinetics, Patient Safety, and Preference (DIET Study). Clinical Pharmacology & Therapeutics 2019, 106 (5), 1076-1082. DOI: https://doi.org/10.1002/cpt.1515.
35. Rini, B. I.; Plimack, E. R.; Stus, V.; Gafanov, R.; Hawkins, R.; Nosov, D.; Pouliot, F.; Alekseev, B.; Soulières, D.; Melichar, B.; et al. Pembrolizumab plus Axitinib versus Sunitinib for Advanced Renal-Cell Carcinoma. The New England journal of medicine 2019, 380 (12), 1116-1127. DOI: 10.1056/NEJMoa1816714
36. Pick, A. M.; Nystrom, K. K. Pazopanib for the treatment of metastatic renal cell carcinoma. Clinical therapeutics 2012, 34 (3), 511-520. DOI: 10.1016/j.clinthera.2012.01.014
37. Suttle, A. B.; Ball, H. A.; Molimard, M.; Hutson, T. E.; Carpenter, C.; Rajagopalan, D.; Lin, Y.; Swann, S.; Amado, R.; Pandite, L. Relationships between pazopanib exposure and clinical safety and efficacy in patients with advanced renal cell carcinoma. British Journal of Cancer 2014, 111 (10), 1909-1916. DOI: 10.1038/bjc.2014.503.
38. Westerdijk, K.; Krens, S. D.; Steeghs, N.; van der Graaf, W. T. A.; Tjwa, E.; Westdorp, H.; Desar, I. M. E.; van Erp, N. P. Real-world data on the management of pazopanib-induced liver toxicity in routine care of renal cell cancer and soft tissue sarcoma patients. Cancer chemotherapy and pharmacology 2024, 93 (4), 353-364. DOI: 10.1007/s00280-023-04615-7
39. Stein, A.; Wang, W.; Carter, A. A.; Chiparus, O.; Hollaender, N.; Kim, H.; Motzer, R. J.; Sarr, C. Dynamic tumor modeling of the dose-response relationship for everolimus in metastatic renal cell carcinoma using data from the phase 3 RECORD-1 trial. BMC cancer 2012, 12, 311. DOI: 10.1186/1471-2407-12-311
40. Maitland, M. L.; Wu, K.; Sharma, M. R.; Jin, Y.; Kang, S. P.; Stadler, W. M.; Karrison, T. G.; Ratain, M. J.; Bies, R. R. Estimation of renal cell carcinoma treatment effects from disease progression modeling. Clinical pharmacology and therapeutics 2013, 93 (4), 345-351. DOI: 10.1038/clpt.2012.263
41. Claret, L.; Mercier, F.; Houk, B. E.; Milligan, P. A.; Bruno, R. Modeling and simulations relating overall survival to tumor growth inhibition in renal cell carcinoma patients. Cancer chemotherapy and pharmacology 2015, 76 (3), 567-573. DOI: 10.1007/s00280-015-2820-x
42. Bonate, P. L.; Suttle, A. B. Modeling tumor growth kinetics after treatment with pazopanib or placebo in patients with renal cell carcinoma. Cancer chemotherapy and pharmacology 2013, 72 (1), 231-240. DOI: 10.1007/s00280-013-2191-0

43. Ouerdani, A.; Struemper, H.; Suttle, A. B.; Ouellet, D.; Ribba, B. Preclinical Modeling of Tumor Growth and Angiogenesis Inhibition to Describe Pazopanib Clinical Effects in Renal Cell Carcinoma. CPT: pharmacometrics & systems pharmacology 2015, 4 (11), 660-668. DOI: 10.1002/psp4.12001
44. Spratt JR., J. S. The rates of growth of skeletal sarcomas. Cancer 1965, 18 (1), 14-24. DOI: https://doi.org/10.1002/1097-0142(196501)18:1<14::AID-CNCR2820180105>3.0.CO;2-T.
45. Wicha, S. G.; Märtson, A. G.; Nielsen, E. I.; Koch, B. C. P.; Friberg, L. E.; Alffenaar, J. W.; Minichmayr, I. K. From Therapeutic Drug Monitoring to Model-Informed Precision Dosing for Antibiotics. Clinical pharmacology and therapeutics 2021, 109 (4), 928-941. DOI: 10.1002/cpt.2202
46. Goutelle, S.; Guidi, M.; Gotta, V.; Csajka, C.; Buclin, T.; Widmer, N. From Personalized to Precision Medicine in Oncology: A Model-Based Dosing Approach to Optimize Achievement of Imatinib Target Exposure. Pharmaceutics 2023, 15 (4). DOI: 10.3390/pharmaceutics15041081
47. Centanni, M.; van de Velde, M. E.; Uittenboogaard, A.; Kaspers, G. J. L.; Karlsson, M. O.; Friberg, L. E. Model-Informed Precision Dosing to Reduce Vincristine-Induced Peripheral Neuropathy in Pediatric Patients: A Pharmacokinetic and Pharmacodynamic Modeling and Simulation Analysis. Clinical pharmacokinetics 2024, 63 (2), 197-209. DOI: 10.1007/s40262-023-01336-1
48. Keizer, R. J.; Dvergsten, E.; Kolacevski, A.; Black, A.; Karovic, S.; Goswami, S.; Maitland, M. L. Get Real: Integration of Real-World Data to Improve Patient Care. Clinical Pharmacology & Therapeutics 2020, 107 (4), 722-725. DOI: https://doi.org/10.1002/cpt.1784.
49. Dibbets, A. C.; Koldeweij, C.; Osinga, E. P.; Scheepers, H. C. J.; de Wildt, S. N. Barriers and Facilitators for Bringing Model-Informed Precision Dosing to the Patient's Bedside: A Systematic Review. Clinical Pharmacology & Therapeutics 2025, 117 (3), 633-645. DOI: https://doi.org/10.1002/cpt.3510.
50. Darwich, A. S.; Ogungbenro, K.; Vinks, A. A.; Powell, J. R.; Reny, J.-L.; Marsousi, N.; Daali, Y.; Fairman, D.; Cook, J.; Lesko, L. J.; et al. Why Has Model-Informed Precision Dosing Not Yet Become Common Clinical Reality? Lessons From the Past and a Roadmap for the Future. Clinical Pharmacology & Therapeutics 2017, 101 (5), 646-656. DOI: https://doi.org/10.1002/cpt.659.
51. Henriksen, J. N.; Andersen, C. U.; Fristrup, N. Therapeutic Drug Monitoring for Tyrosine Kinase Inhibitors in Metastatic Renal Cell Carcinoma. Clin Genitourin Cancer 2024, 22 (3), 102064. DOI: 10.1016/j.clgc.2024.102064
52. Mueller-Schoell, A.; Groenland, S. L.; Scherf-Clavel, O.; van Dyk, M.; Huisinga, W.; Michelet, R.; Jaehde, U.; Steeghs, N.; Huitema, A. D. R.; Kloft, C. Therapeutic drug monitoring of oral targeted antineoplastic drugs. European journal of clinical pharmacology 2021, 77 (4), 441-464. DOI: 10.1007/s00228-020-03014-8
53. Westerdijk, K.; Desar, I. M. E.; Steeghs, N.; van der Graaf, W. T. A.; van Erp, N. P. Imatinib, sunitinib and pazopanib: From flat-fixed dosing towards a pharmacokinetically guided personalized dose. British journal of clinical pharmacology 2020, 86 (2), 258-273. DOI: 10.1111/bcp.14185

SUPPLEMENTAL MATERIAL

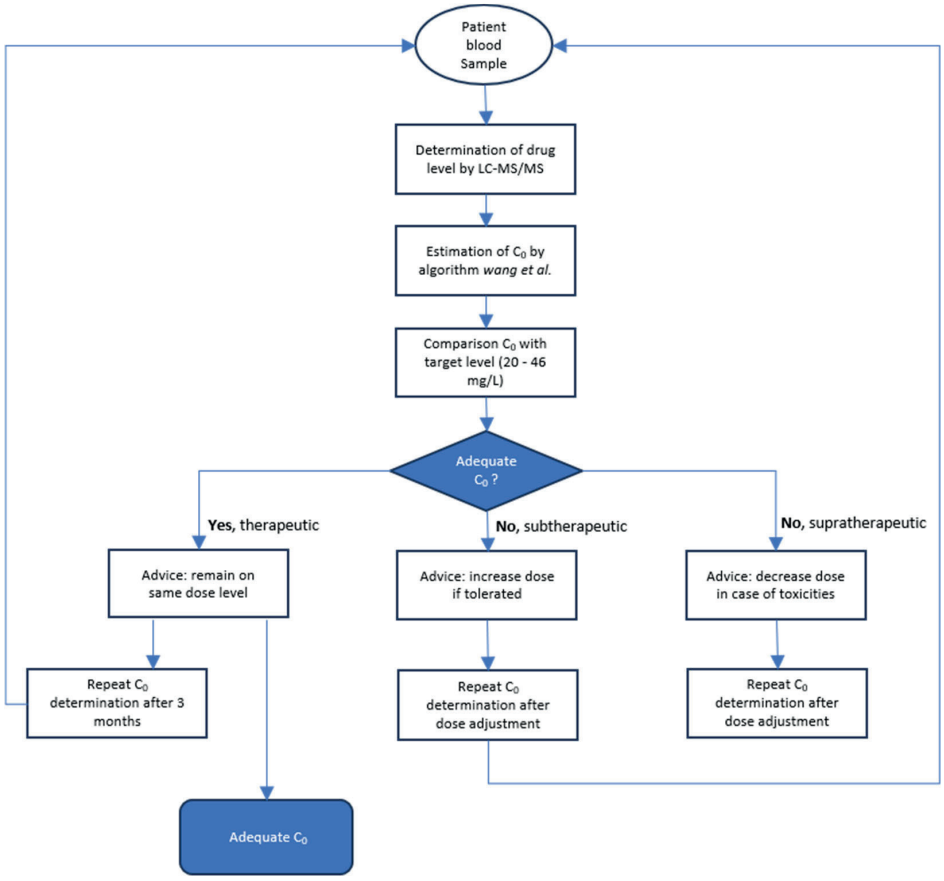

Figure S4.1. TDM routine practice workflow and dose adjustment algorithms.

Dose adjustments were advised as follows:
If the (estimated) trough level is too low: preferably increase the reversal dose in steps of 200 mg and repeat the trough level 2 weeks after dose change. At doses > 800 mg, it is generally considered not useful to increase the times dosage further. Then consider increasing the level by means of simultaneous intake with food (breakfast) or splitting the daily dose into 2 dd 400 mg. In case of a trough level in the therapeutic window: maintain dosage if toxicity is acceptable. In case of high trough levels: in case of toxicity, reduce dose so that level is within therapeutic window (200/400 mg increments), repeat trough level 2 weeks after dose change.

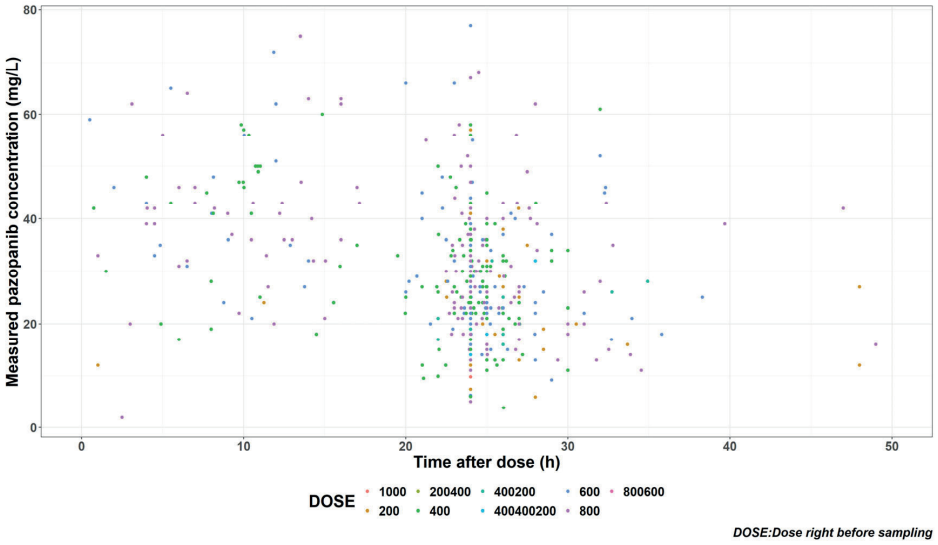

Figure S4.2. Raw data of measured pazopanib concentration versus time after dose. 400200/200400: 400 mg once and 200 mg once switch every day; 800600: 800 mg once and 600 mg once switch every day; 400400200: 400 mg once for 2 days followed by 200 mg once for 1 day.

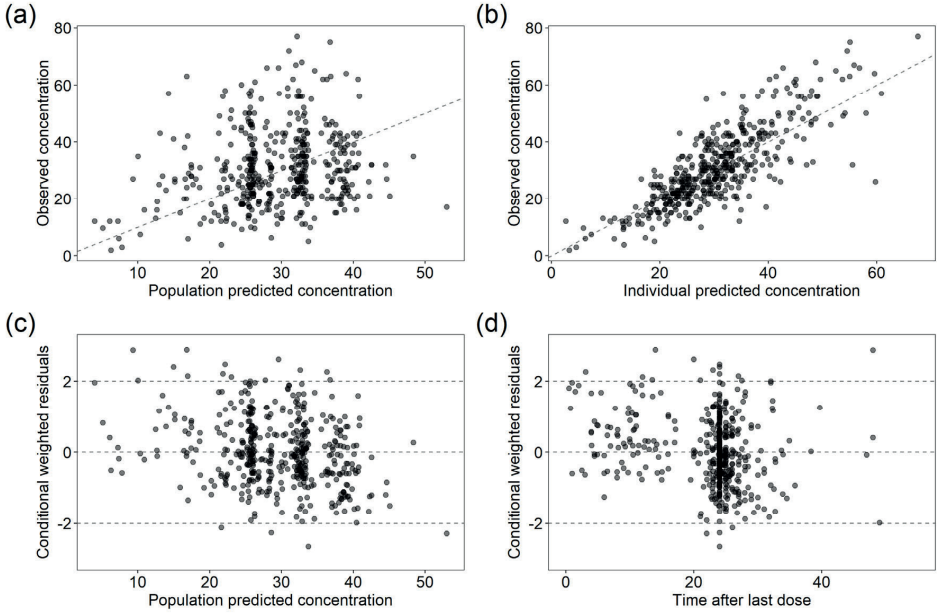

Figure S4.3. Goodness-of-fit plot of pazopanib final POPPK model.

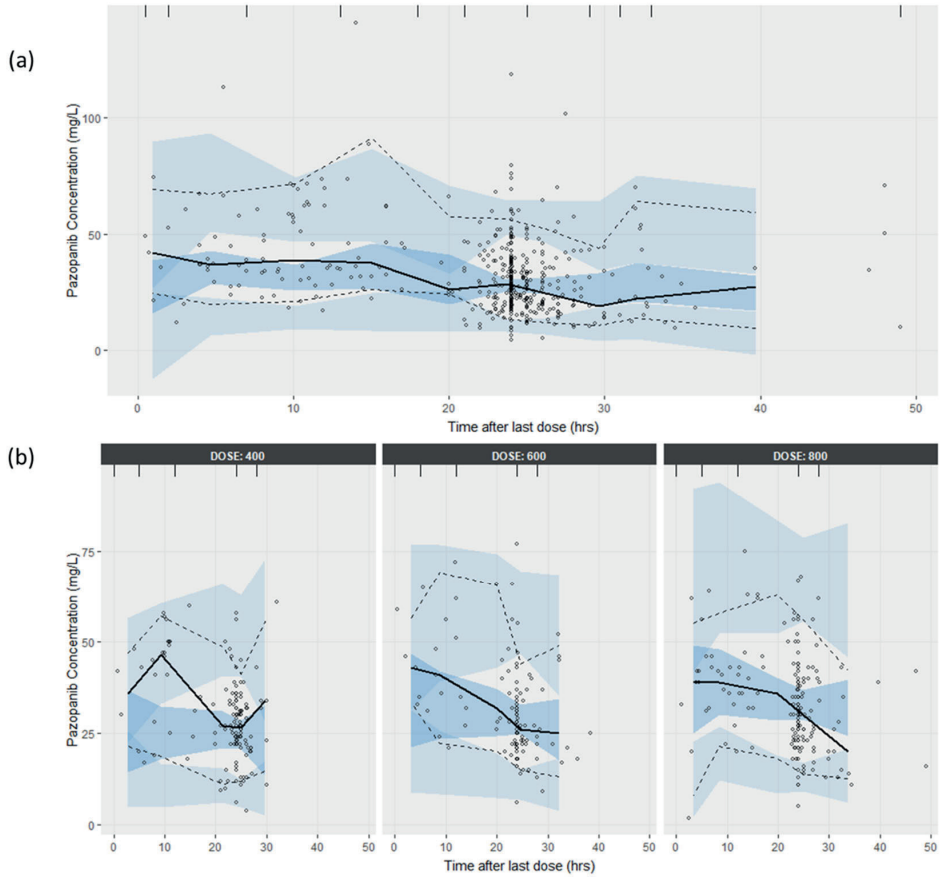

Figure S4.4. Prediction-corrected Visual Predictive Check of pazopanib final POPPK model of **(a)** all data; **(b)** stratified by DOSE.

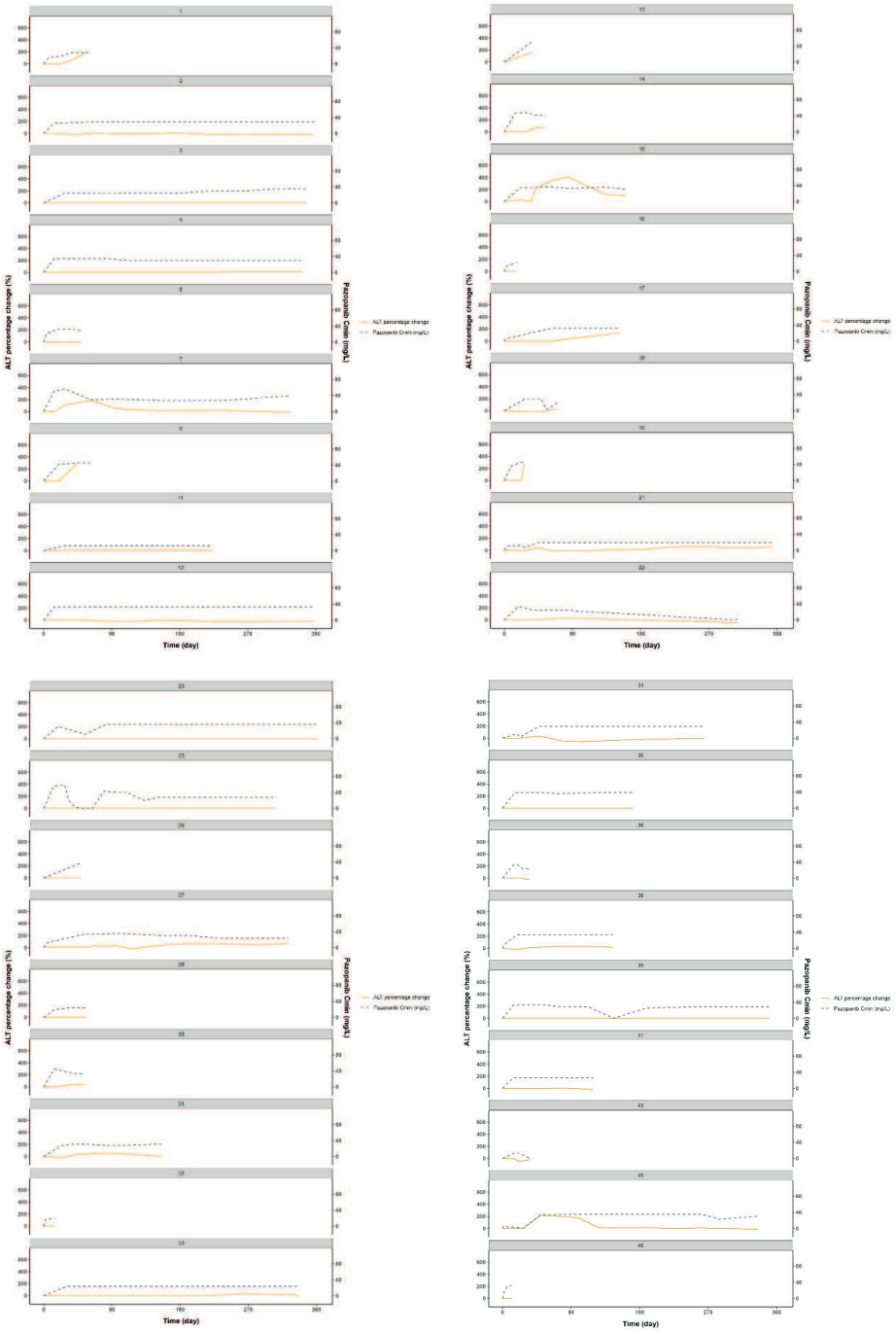

Figure S4.5. Toxicity raw data exploration of the percentage change of liver enzyme (yellow line) over time and pazopanib predicted trough concentration over time (dashed black line) after pazopanib treatment initiation of each individual. *Figure continues on next page.*

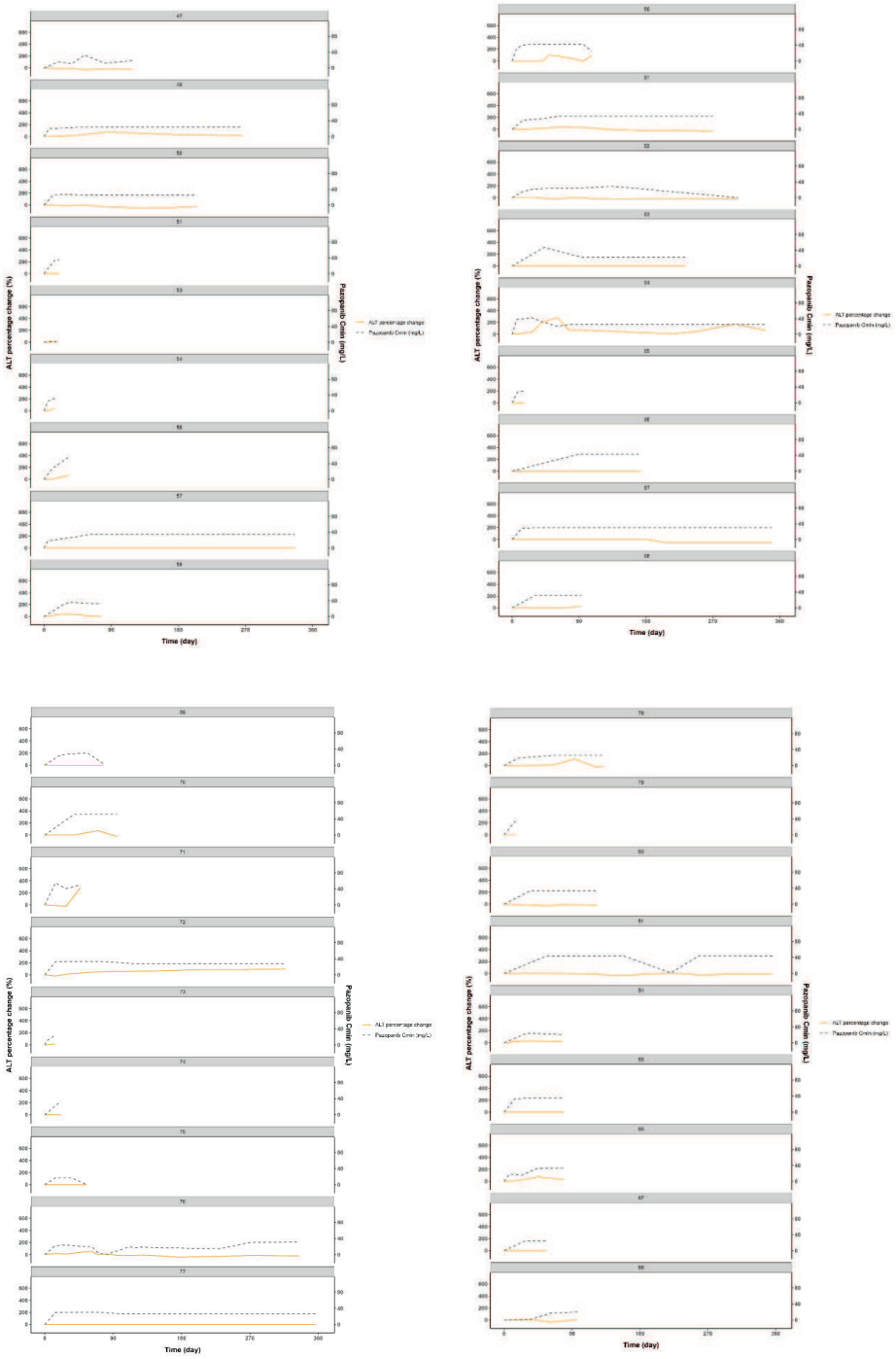

Figure S4.5. *Continued.*

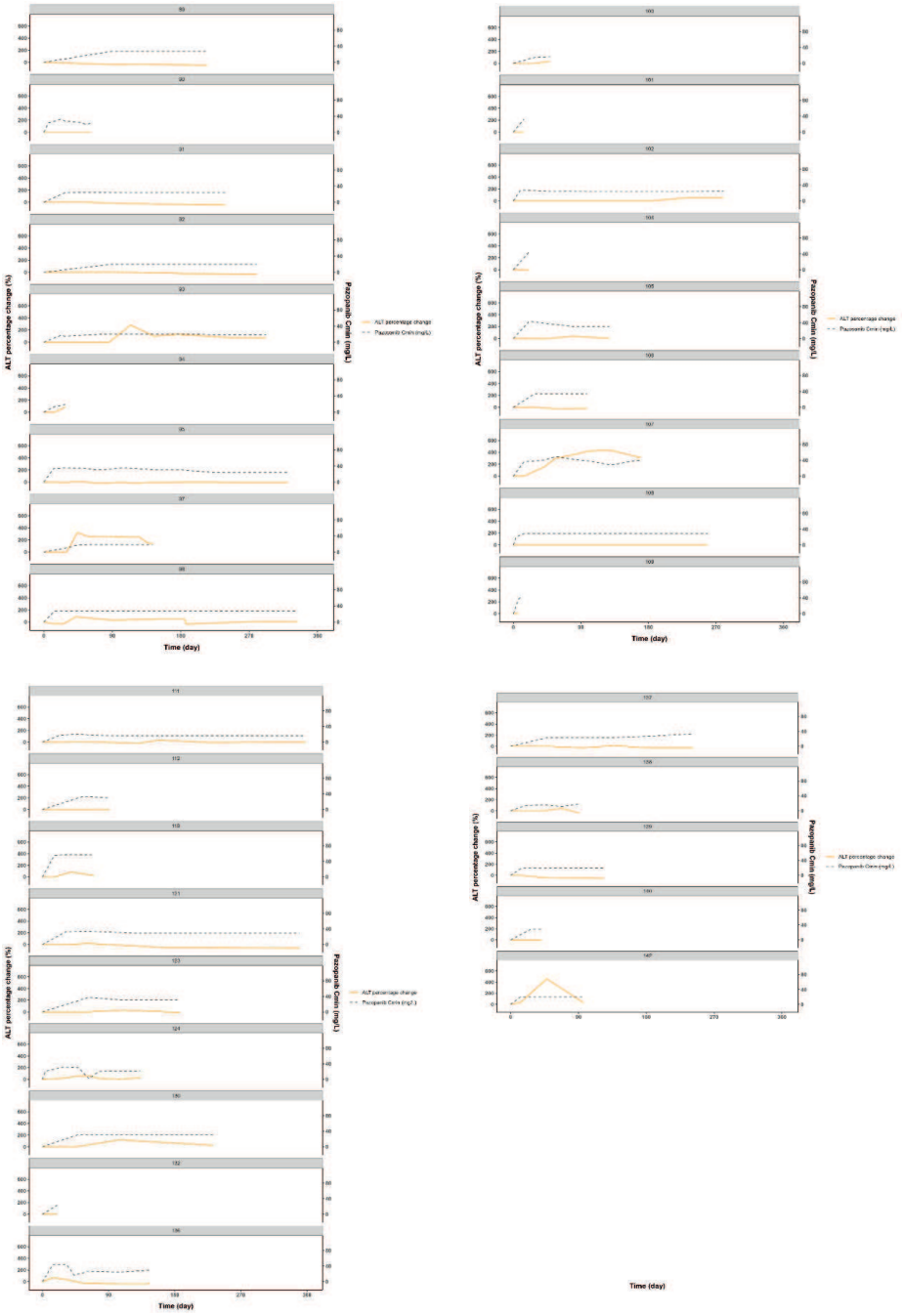

Figure S4.5. *Continued.*

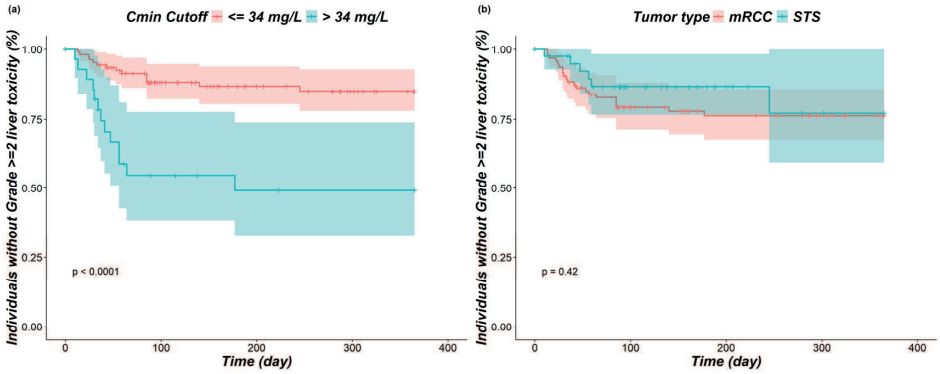

Figure S4.6. Kaplan-Meier plot of the observed Grade ≥ 2 liver toxicity free probability over one year censoring time stratified by (a) trough concentration of 34 mg/L and (b) tumor types. The lines represent the observations at event or right-censoring time. The vertical lines represent the censored observations.

Table S4.1. Selection of $C_{min,ss}$ cutoff of TTE model

Cutoff $C_{min,ss}$ (mg/L)	HR [exp(coef)] (RSE%)	dOFV (compare with base model)
> 20.5 (the current efficacy threshold)	1.28 (204)	-0.25
> 31	3.15 (35%)	-8.75
> 32	2.77 (38%)	-6.93
> 33	2.59 (40%)	-5.95
> 34	3.35 (32%)	-9.13
> 35	4.22 (27%)	-12.67
> 36	4.76 (25%)	-14.57
> 37	4.10 (28%)	-11.04
> 38	4.62 (26%)	-12.76
> 39	5.37 (23%)	-15.17
> 40	4.48 (27%)	-10.81
> 41	5.16 (25%)	-12.51
> 42	4.10 (31%)	-7.95
> 43	3.63 (36%)	-5.99

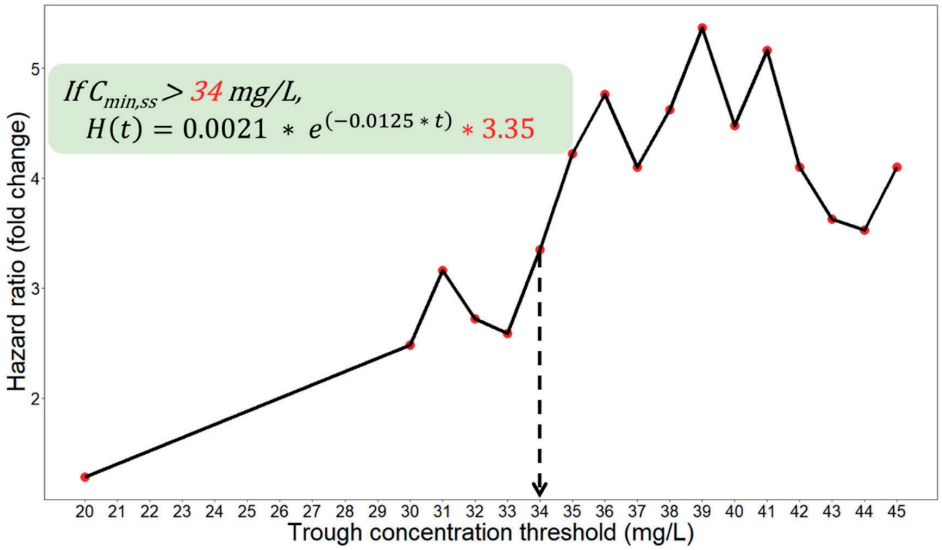

Figure S4.7. The liver toxicity hazard ratio fold change of different $C_{min,ss}$ cutoff. Dotted vertical line indicated the $C_{min,ss}$ > 34 mg/L threshold.

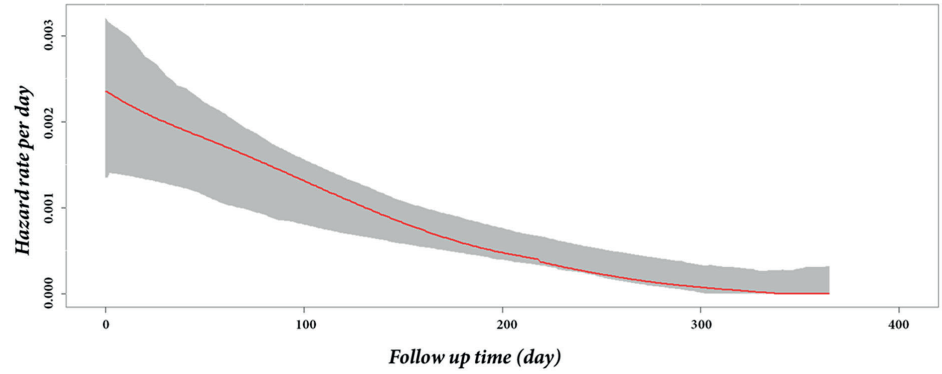

Figure S4.8. Hazard-based visual prediction check of final TTE liver toxicity model. The red line represents the observed hazard estimates derived from non-parametric hazard estimator. The shaded area represents the 90% prediction interval of simulated hazard estimates derived from non-parametric hazard estimator.

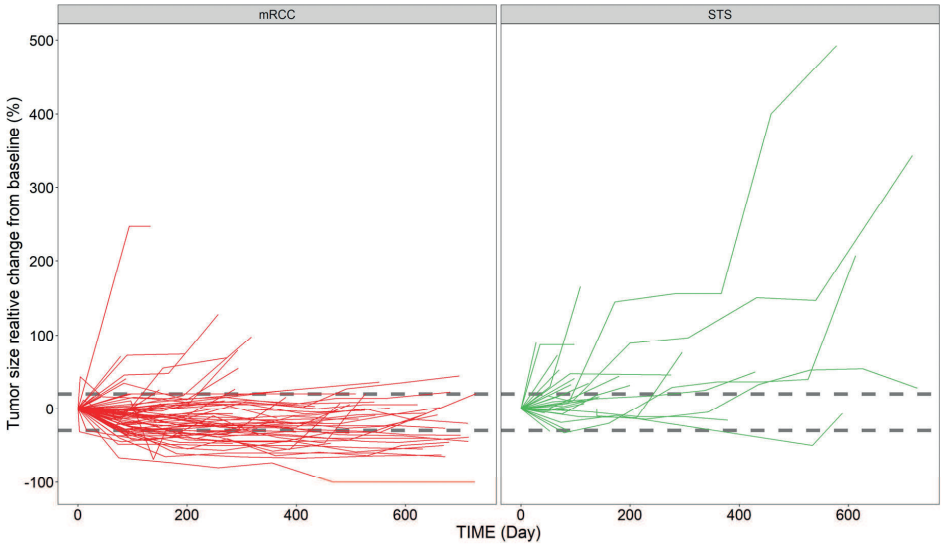

Figure S4.9. Raw data of collected TS dynamics data. The dashed lines represent the interval of stable disease according to RECIST1.1 criteria that tumor size relative change from -30% to +20% when compared with the baseline tumor size.

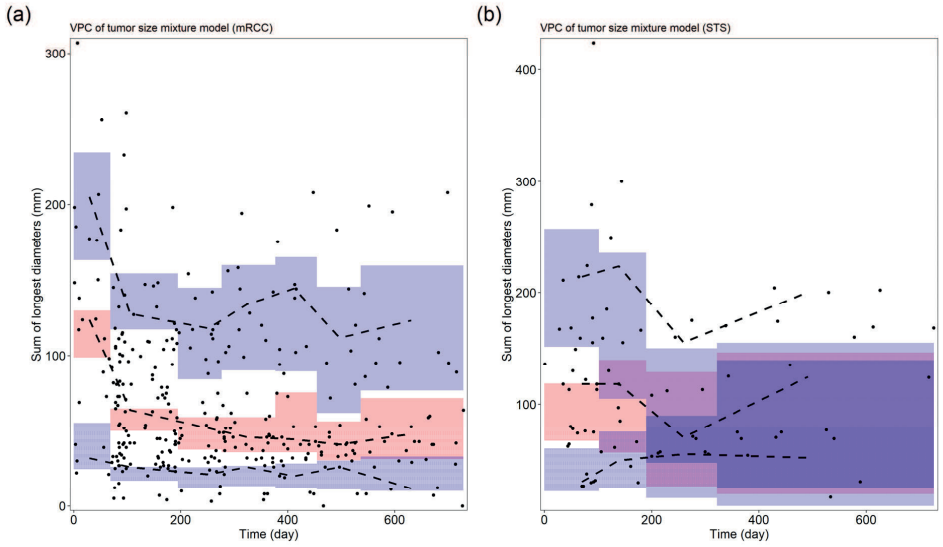

Figure S4.10. Prediction-corrected visual predictive check of final TS dynamics model. Black dots indicate real observations. Black dashed lines represent 95th, 50th and 5th percentiles of the observations. The blue shaded areas represent 95% confidence interval of the 95th and 5th percentiles based on the simulations respectively, and the red shaded area represents 95% confidence interval of the 50th percentile based on the simulations.

Figure S4.11. Interface of the R shiny pazopanib dose optimization application updated from Le Louedec et al. Dose adjustment recommendations can be generated according to the randomly collected sample. The dose information, time after last dose information can be provided in left panel. Right panels are dataset for Maximum a posterior Bayesian estimation and simulations, predicted concentration over time, individual ETA distribution and alternative regimens simulated $C_{min,ss}$. *Figure continues on next page.*

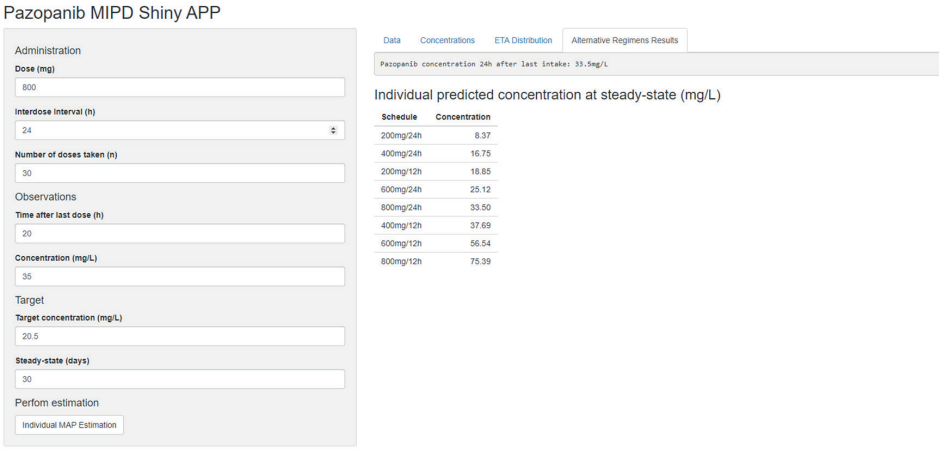

Figure S4.11. *Continued.*

NONMEM Code: PK model; TTE model; Tumor size model

Pazopanib POPPK model control stream

```
$INPUT C ID TIME ADDL DV AMT II CMT EVID Sex Age WT HT BMI TT Food COMED DOSE
TAD OC1 OC2
$SUBROUTINES ADVAN2 TRANS2

$PK
IF(AMT.GT.0) THEN
TDOS=TIME
ENDIF
IF (AMT.GT.0) THEN
DOS = AMT
ENDIF
FCOV=(200/DOS)**THETA(7)
CL = THETA(1)
V = THETA(2) * EXP(ETA(1))
KA = THETA(3)
F1 = THETA(6)*EXP(ETA(2)) *FCOV
S2 = V

$ERROR
IPRED = F
W = SQRT(THETA(4)**2*IPRED**2 + THETA(5)**2)
Y = IPRED + W*EPS(1)
IRES = DV-IPRED
IWRES = IRES/W

$THETA
(0.497) ; CL
(46.1) ; V
(0.976) FIX ; KA
(0.24) ; Prop.RE (sd)
(4.71) ; Add.RE (sd)
(1) FIX ; F1
(0.42) ; FCOV

$OMEGA
0.58 ; IIV V
0.12 ;IIV F1

$SIGMA
1 FIX
$EST METHOD=1 POSTHOC INTER MAXEVAL=9999 NOABORT SIG=3 PRINT=1
$COV UNCONDITIONAL PRINT=E MATRIX=R
```

Pazopanib liver toxicity TTE model control stream

```
$INPUT C ID TIME DV EVID Galt Gast Gaf Sex Age WT HT BMI TT FOOD COMED DOSE
ICL IV IKA AUC CONC1 FDOSE FLAG trough max number AUC24 OLDTIME CUTOFF
$SUBROUTINES ADVAN=13 TOL=9
$MODEL COMP=(HAZARD)

$PK
TP=0
CL = ICL
V = IV
KA = IKA
LAM = THETA(1)*EXP(ETA(1))
SHP = THETA(2)
RF=1
IF(trough.GT.34) RF = EXP(THETA(3))

$DES
DADT(1) = LAM*RF*EXP(SHP*T)

$ERROR
IF(NEWIND.NE.2) OLDCHZ=0
CHZ = A(1) - OLDCHZ
;Sim_start
OLDCHZ=0
;Sim_end
SURX = EXP(-CHZ)
HAZNOW = LAM*RF*EXP(SHP*TIME)
IF(DV.EQ.0) Y=SURX
IF(DV.EQ.1) Y=SURX*HAZNOW
IF(ICALL.EQ.4) THEN
CALL RANDOM (2,R)
DV=0
RTTE=0
IF(EVID.EQ.0) RTTE=1
IF(R.GT.SURX) THEN
DV=1
RTTE=1
ENDIF
ENDIF

$THETA
(0.0021) ; LAMDA
(-0.012) ; SHAPE
(1.21) ; Cmin COEFFICIENT
```

```
$OMEGA
0 FIX
;Sim_start
;$SIM (1234) (2345 UNIFORM) ONLYSIM NOPREDICTION NSUB=100

$ESTIM MAXEVAL=9999 METHOD=0 LIKE SIGL=9 NSIG=3 PRINT=1
$COV PRINT=E MATRIX=R
;Sim_end
```

Pazopanib tumor size dynamics model control stream for mRCC

```
$INPUT C ID TIME=DROP TIMEDAY=TIME DV AMT II CMT EVID ADDL TAD FLAG Sex
Age WT HT BMI TT Food COMED DOSE BASE BASERENAL ET CL Vc Ka CONC1 AUC24
trough max RESP
$SUBROUTINE ADVAN13 TOL=4
$MODEL
COMP=(drug)
COMP=(conc)
COMP=(TS)
$MIX
P(1) = THETA(7)
P(2) = 1.0-THETA(7)
NSPOP=2

$PK
KG = THETA(1)*EXP(ETA(1))
IF(MIXNUM.EQ.2) THEN
KD = THETA(2)
ELSE
KD = THETA(3) *EXP(ETA(2))
ENDIF
BESTSUB=MIXEST
LAMDA = THETA(6)*EXP(ETA(3))

k20 = CL/Vc
S3=1
AUC = DOSE/CL

A_0(1)= 0
A_0(2)= 0
A_0(3)= BASE

$DES
DADT(1) = -Ka*A(1)
DADT(2) = Ka*A(1)-k20*A(2)
DADT(3) = KG*A(3)-KD*EXP(-lamda*T)*A(3) ; yes/no drug effect

$ERROR
A1=A(1)
A2=A(2)
A3=A(3)
IPRED = A3
W = SQRT(THETA(4)**2*IPRED**2 + THETA(5)**2)
Y = IPRED + W*EPS(1)
```

```
IRES = DV-IPRED
IWRES = IRES/W

$THETA
(0.0005) ; KG
(0) FIX ;KD
(0.004) ; KD1
(0.138) ; Prop.RE (sd)
(1.24) ; Add.RE (sd)
(0.008) ; lamda
(0.73) ; PROPORTION

$OMEGA
1.69 ;IIV KG
0.29 ;IIV KD
0 FIX ; IIV lamda

$SIGMA
1 FIX

$EST METHOD=1 INTER MAXEVAL=5000 NOABORT NSIG=2 SIGL=9 PRINT=5 NOTHETA-
BOUNDTEST POSTHOC ETASAMPLES=1 ISAMPLE=100 EONLY=1
$COV PRINT=E UNCONDITIONAL MATRIX=S
```

Pazopanib tumor size dynamics model control stream for STS

```
$INPUT C ID TIME=DROP TIMEDAY=TIME DV AMT II CMT EVID ADDL TAD FLAG Sex
Age WT HT BMI TT Food COMED DOSE BASE BASERENAL ET CL Vc Ka CONC1 AUC24
trough max RESP
$SUBROUTINE ADVAN13 TOL=4
$MODEL
COMP=(drug)
COMP=(conc)
COMP=(TS)

$MIX
P(1) = THETA(7)
P(2) = 1.0-THETA(7)
NSPOP=2

$PK
KG = THETA(1)*EXP(ETA(1))
IF(MIXNUM.EQ.2) THEN
KD = THETA(2)
ELSE
KD = THETA(3) *EXP(ETA(2))
ENDIF
BESTSUB=MIXEST
LAMDA = THETA(6)*EXP(ETA(3))

k20 = CL/Vc
S3=1
AUC = DOSE/CL

A_0(1)= 0
A_0(2)= 0
A_0(3)= BASE

$DES
DADT(1) = -Ka*A(1)
DADT(2) = Ka*A(1)-k20*A(2)
DADT(3) = KG*A(3)-KD*EXP(-lamda*T)*A(3)

$ERROR
A1=A(1)
A2=A(2)
A3=A(3)

IPRED = A3
W = SQRT(THETA(4)**2*IPRED**2 + THETA(5)**2)
```

```
Y = IPRED + W*EPS(1)
IRES = DV-IPRED
IWRES = IRES/W

$THETA
(0.0086) ; KG
0 FIX ;KD
(0.008) ; KD1
(0.166) ; Prop.RE (sd)
(8.1) ; Add.RE (sd)
(0.0003) ; lamda
(0.866) ; PROPORTION

$OMEGA
0 FIX ;IIV KG
0.017 ;IIV KD
0 FIX ; IIV lamda

$SIGMA
1 FIX

$EST METHOD=1 INTER MAXEVAL=9999 NOABORT NSIG=2 SIGL=9 PRINT=5 NOTHETA-
BOUNDTEST POSTHOC
$COV PRINT=E UNCONDITIONAL MATRIX=S
```